

Persistence of a reef fish metapopulation via network connectivity: theory and data

Allison G. Dedrick^{a,*}

Katrina A. Catalano^a

Michelle R. Stuart^a

J. Wilson White^b

Humberto Montes, Jr.^c

Malin Pinsky^a

a. Department of Ecology Evolution and Natural Resources, Rutgers University, 14
College Farm Road, New Brunswick, NJ 08901 USA;

b. Department of Fisheries and Wildlife, Coastal Oregon Marine Experiment Sta-
tion, Oregon State University, Newport, OR 97365 USA;

c. Visayas State University

* Corresponding author; e-mail: agdedrick@gmail.com

(Author order not yet determined)

Introduction

Metapopulation dynamics and persistence depend on connectivity among patches
3 and the demographic rates at each patch (e.g. Hastings and Botsford, 2006; Hanski,
1998). Assessing levels of connectivity and demographic parameters has been par-
ticularly challenging for marine species, where much of the mortality and movement
6 happens at larval and juvenile stages when individuals are hard to track and have
the potential to travel long distances with ocean currents (reviewed in White et al.,
2019). A need to understand metapopulations for conservation and management,
9 such as siting marine protected areas (e.g. Botsford et al., 2001; White et al., 2010),
however, has led to a large body of theory describing how marine metapopulations
might persist.

12 For any population to persist, individuals must on average replace themselves
during their lifetime. Assessing replacement must take into account the demographic
processes across the whole life cycle, including how likely individuals are to survive to
15 the next age or stage, their expected fecundity at each stage, and the survival of any
offspring produced to recruitment. In a spatially structured population, as many
marine populations are, in addition to assessing whether the reproductive output
18 and survival of a population is sufficient, we must also consider how the offspring are
distributed across space.

Considering both the demographic processes within patches and the connectivity
21 among them, a metapopulation can persist in two ways: 1) at least one patch can
achieve replacement in isolation, or 2) patches receive enough recruitment to achieve

replacement through multi-generational loops of connectivity with other patches in
24 the metapopulation (Hastings and Botsford, 2006; Burgess et al., 2014). In the first
case (termed self-persistence), enough of the reproductive output produced at one
patch is retained at the patch for it to persist. In the second (network persistence),
27 closed loops of connectivity among at least some of the patches - where individuals
from one patch settle at another and eventually send offspring back to the first in a
future generation - provide the patch with enough recruitment to persist within the
30 network. Though it has been challenging to estimate the parameters necessary to
understand how actual metapopulations persist, a large work of theory developed in
part to guide marine protected area design helps predict when each type of persistence
33 is likely to occur (i.e., habitat patches or protected areas that are large relative to
the mean dispersal distance are likely to be self-persistent, White et al., 2010).

New ways of identifying individuals and determining their origins, such as otolith
36 and shell microchemistry and genetic parentage analysis (e.g. Wang, 2004, 2014), now
allow us to better measure dispersal (e.g. Almany et al., 2017; D'Aloia et al., 2013)
and a better appreciation of the relevant population dynamic theory has led to mea-
39 surement of the appropriate demographic factors (e.g. Carson et al., 2011; Hameed
et al., 2016) necessary to assess persistence in real metapopulations. We might ex-
pect that populations on isolated islands are the most likely to be self-persistent, as
42 they lack nearby populations with which to exchange larvae and would go locally
extinct if they did not achieve replacement. At isolated Kimbe Island in Papua New
Guinea, Salles et al. (2015) find that the population of orange clownfish (*Amphiprion*
45 *percula*) can likely persist without outside immigration. In contrast, populations of

bicolor damselfish (*Stegastes partitus*) at four study sites nested within a larger reef metapopulation in the Bahamas do not appear able to persist without outside input
48 (Johnson et al., 2018). Persistence has yet to be assessed in the field for an entire marine metapopulation, such as all of the patches in a coastal metapopulation.

The number of studies estimating demographic rates and connectivity in marine
51 metapopulations is growing (e.g. Carson et al., 2011; Salles et al., 2015; Johnson et al., 2018; Garavelli et al., 2018), but most use data from one or a few years. Longer data sets enable better estimates of long-term average rates, rather than
54 assuming the demographic and dispersal rates from a particular year or two are representative. Long data set are also useful for explicitly considering uncertainty, both to assess how well we understand persistence for a population and to assess
57 which parameters contribute most to our uncertainty. Finally, sampling over many years provides abundance trends to compare with persistence metrics.

Here, we further our understanding of metapopulation dynamics in a network
60 of patches along a coastline through a study of yellowtail clownfish (*Amphiprion clarkii*) in the Philippines. We assess persistence for all patches of habitat within a 30 km stretch of coastline, exceeding estimates of the dispersal spread for this species
63 (Pinsky et al., 2010), suggesting the network is likely to operate as a contained metapopulation. With seven years of annual sampling data, we are able to estimate persistence metrics and replacement over the longer term and investigate abundance
66 through time to compare with the replacement-based persistence metrics. We use our long-term data set from habitat patches on a continuous section of coastline to understand persistence within a local network. We find that our sites have stable

⁶⁹ abundances through time but are unlikely to persist as an isolated metapopulation
and require immigration from outside patches to persist.

Methods

⁷² Persistence theory and metrics

For a population to persist, each individual must on average replace itself (e.g. Hastings and Botsford, 2006; Botsford et al., 2019). In non-spatially structured populations, we use criteria such as the average number of recruiting offspring each individual produces during its life (called R_0 when the population is age-structured and density-independent) or the growth rate of the population (such as the dominant eigenvalue λ of an age-structured Leslie matrix) (Caswell, 2001; Burgess et al., 2014). For spatially-structured populations, we must also consider the spatial spread of offspring, often represented through a dispersal kernel or connectivity matrix (Burgess et al., 2014).

We consider four primary metrics to assess whether and how the population is persistent: 1) lifetime recruit production (LRP), to assess whether the population has enough surviving offspring to achieve replacement, 2) self-persistence (SP), to assess whether any individual patch can persist in isolation without input from other patches, 3) network persistence (NP), to assess whether the metapopulation is persistent as a connected unit, and 4) local replacement (LR), as second assessment of whether individuals replace themselves with recruits retained within population. We explain each metric below in detail. To represent the uncertainty in our estimates, we

⁹⁰ calculate each metric 1000 times, sampling each input parameter from a distribution
that represents the uncertainty in each empirical estimate of demographic rates or
connectivity. In our results, we show our best estimate of each persistence metric
⁹³ along with the range of uncertainty values.

Lifetime recruit production

We find the estimated number of recruits an individual recruit will produce (lifetime
⁹⁶ recruit production: LRP) by multiplying the total number of eggs a recruit-sized
individual will produce in its lifetime (lifetime egg production: LEP) by the fraction
of those eggs that will survive to become recruits (egg-recruit survival: S_e) (Fig. 1):

$$\text{LRP} = \text{LEP} * S_e. \quad (1)$$

⁹⁹ If $\text{LRP} \geq 1$, the population has the potential for replacement; individuals produce
enough surviving offspring, before considering dispersal. If $\text{LRP} < 1$, the individuals
are not replacing themselves and the population cannot persist without input from
¹⁰² outside patches and is a sink habitat within a larger metapopulation (Pulliam, 1988).
We use all recruits produced by adults in our population to estimate LRP , regardless
of where they settle.

¹⁰⁵ Self-persistence

A patch is able to persist in isolation (self-persistent) if individuals produce enough
offspring that survive to recruitment (LRP) and settle in the natal patch (i , with

¹⁰⁸ probability of dispersal $p_{i,i}$) to replace themselves:

$$SP_i = \text{LRP}_i \times p_{i,i}. \quad (2)$$

A patch i is self-persistent if $SP_i \geq 1$. If at least one patch is self-persistent, the metapopulation as a whole is persistent as well (Hastings and Botsford, 2006; ¹¹¹ Burgess et al., 2014). Our equation for SP is a modification of that used in Burgess et al. (2014), which uses LEP to represent offspring produced and uses local retention (the number of surviving recruits that disperse back to the natal patch divided by ¹¹⁴ the number of eggs produced by the natal patch) to capture egg-recruit survival and dispersal combined: $\text{LEP} \times \text{local retention} \geq 1$. We modify this to include egg-recruit survival in the offspring term instead, using LRP in place of LEP.

¹¹⁷ **Network persistence**

Network persistence explicitly considers dispersal of individuals among sites, a critical part of the larval life stage, in addition to the reproduction and survival at each ¹²⁰ site. We represent dispersal with a dispersal kernel, which relates the likelihood of an individual dispersing to the distance traveled. We find the probabilities of a recruit dispersing between each set of sites ($p_{i,j}$) by integrating the dispersal kernel ¹²³ over the distances between sites. We then create a realized connectivity matrix C by multiplying the dispersal probabilities by the expected number of recruits an individual produces: $C_{i,j} = \text{LRP} \times p_{i,j}$ (Burgess et al., 2014, though we include egg-

¹²⁶ recruit survival in LRP, rather than in $p_{i,j}$ as they do). The diagonal entries of C , where the origin and destination are the same site, are the values of self-persistence for each individual site.

¹²⁹ Network persistence evaluates the largest real eigenvalue of the realized connectivity matrix λ_C , which must be greater than 1 for the network to persist without outside input: $NP = \lambda_C \geq 1$ (e.g. Hastings and Botsford, 2006; White et al., 2010; ¹³² Burgess et al., 2014).

Local replacement

Like network persistence, local replacement (LR) assesses whether the population ¹³⁵ is locally self-sustaining. Rather than considering dispersal explicitly as network persistence does, local replacement modifies LRP to estimate the average number of recruits produced per individual that return to settle within our sites. We estimate ¹³⁸ LR by multiplying LEP by the proportion of eggs produced that survive and return to recruit at our sites (R_e), a modification of egg-recruit survival that implicitly includes dispersal. If $LR \geq 1$, individuals produce enough locally-retained offspring ¹⁴¹ to replace themselves and the population can persist in isolation.

$$LR = LEP \times R_e. \quad (3)$$

Study system

We focus on a tropical metapopulation of yellowtail clownfish (*Ampiprion clarkii*, Fig. ¹⁴⁴ 2c) on the west coast of Leyte island facing the Camotes Sea in the Philippines (Fig.

2a). Like many clownfish species, yellowtail clownfish have a mutualistic relationship with anemones that house small colonies of fish (Buston, 2003b; Fautin et al., 1992).

147 Yellowtail clownfish are protandrous hermaphrodites and maintain a size-structured hierarchy; within an anemone, the largest fish is the breeding female, the next largest is the breeding male, and any smaller fish are non-breeding juveniles. The fish
150 move up in rank to become breeders only after the larger fish have died. In the tropical patch reef habitat of the Philippines, yellowtail clownfish primarily spawn from November to May, laying clutches of benthic eggs that the parents protect and
153 tend (Ochi, 1989; Holtswarth et al., 2017). Larvae hatch after about six days and spend 7-10 days in the water column before returning to reef habitat to settle in an anemone (Fautin et al., 1992).

156 Clownfish are particularly well-suited to metapopulation studies due to their limited movement as adults and well-defined patchy habitat. Once fish have settled, they tend to stay within close proximity of their anemones, which are found on reef
159 patches. This makes fish easier to relocate for mark-recapture studies and simplifies the exchange between patches to only dispersal during the larval phase. Patches, whether considered to be the reef patch or the anemone territory of the fish, are
162 discrete and easily delineated (Fig. 2a, b), which makes determining the spatial structure of the metapopulation clear. Additionally, clear patches make it easier to assess how much of the site has been surveyed. These simplifying characteristics in habitat and fish behavior make clownfish and other similarly territorial reef
165 fish useful model systems for studies of metapopulation dynamics and persistence (e.g. Buston and DAloia, 2013; Salles et al., 2015; Johnson et al., 2018). Our fo-

¹⁶⁸ cal species of yellowtail clownfish tends to behave more like larger reef fishes, with
wider-ranging territories and stronger swimming abilities (Hattori and Yanagisawa,
1991; Ochi, 1989), than the smaller clownfish *A. percula* commonly used in previous
¹⁷¹ metapopulation studies (e.g. Buston et al., 2011; Salles et al., 2015). As we show
later, survival in yellowtail clownfish is also lower than *A. percula* and more similar
to other damselfishes. MAKE SURE THIS SENTENCE IS TRUE!

¹⁷⁴ **Field data collection**

We focus on a set of nineteen patch reef sites spanning 30 km along the western coast
of Leyte island (Fig. 2a). The sites consist of rocky patches of coral reef separated
¹⁷⁷ by sand flats, with reef patches covering approximately 20% of the sampling region
(Fig. 2b). On the north edge, the sites are isolated from nearby habitat with no
substantial reef habitat for at least 20 km.

¹⁸⁰ Since 2012, we have sampled fish and habitat at most of the sites annually (Table
A2). During sampling, divers using SCUBA and tethered to GPS readers swam the
extent of each site. Divers visited each anemone inhabited by yellowtail clownfish
¹⁸³ and tagged anemones. At each anemone, the divers attempted to catch all of the
yellowtail clownfish 3.5 cm and larger, took a small tail fin-clip from each for use in
genetic analysis, measured the fork length, and noted the tail color (as an indicator of
¹⁸⁶ life stage). Starting in the 2015 field season, fish 6.0 cm and larger were also tagged
with a passive integrated transponder (PIT) tag, unless already tagged. Divers also
looked for eggs around each anemone and measured and photographed any clutches
¹⁸⁹ found. In total, we took fin clips from and genotyped 2407 fish and PIT-tagged 1930

fish across all years and sites combined, marking 3053 individual fish.

192 Estimating demographic and dispersal parameters from empirical data

Parentage analysis and dispersal kernel

Over seven years of sampling, we genotyped 1719 potential parents and 785 juveniles
195 and found 62 parent-offspring matches (details in Catalano et al., in prep). We use a distance-based dispersal kernel fit from the parent-offspring matches (Catalano et al.,
in prep), where the relative dispersal $p(d)$ is a function of distance d in kilometers and
198 parameters $\theta = 1.19$ and $z = e^{k_d=-2.33}$ that control the shape and scale of the kernel:
 $p(d) = ze^{-(zd)^\theta}$. The dispersal kernel estimates the relative dispersal by distance for fish that have survived and recruited so does not estimate pre-settlement mortality.
201 To find the probability of fish dispersing among our sites, we numerically integrate the dispersal kernel using the distance from the middle of the origin site (i) to the closest (d_1) and farthest (d_2) bounds of the destination site (j):

$$p_{i,j}(d) = \int_{d_1}^{d_2} ze^{-(zd)^\theta} dd. \quad (4)$$

204 To account for uncertainty in the dispersal kernel, we use sets of the shape parameter θ and the scale parameter k_d that represent the span of the 95% confidence interval when k_d and θ are estimated jointly (Catalano et al., in prep).

207 **Growth and survival: mark-recapture analyses**

We marked fish with both genetic samples and PIT tags, allowing us to estimate growth and survival through mark-recapture. In total, we have 3053 marked fish
210 with size and stage data for each capture time.

For growth, we estimated the parameters of a von Bertalanffy growth curve (Fabens, 1965) in the growth increment form relating the length at first capture
213 L_t to the length at a later capture L_{t+1} (Hart and Chute, 2009), where L_∞ is the average asymptotic size across the population and K controls the rate of growth:

$$\begin{aligned} L_{t+1} &= L_t + (L_\infty - L_t)[1 - e^{(-K)}] \\ &= e^{(-K)}L_t + L_\infty[1 - e^{(-K)}]. \end{aligned} \tag{5}$$

We see from eqn. 5 that we would expect the first length L_t and the second length
216 L_{t+1} to be related linearly (Hart and Chute, 2009). From the slope $m = e^{(-K)}$ and y-intercept $b = L_\infty[1 - e^{(-K)}]$, we calculated the von Bertalanffy parameters, such that $K = -\ln m$ and $L_\infty = \frac{b}{(1-m)}$. We used the first and second capture lengths
219 for fish that were recaptured after a year (within 345 to 385 days) to estimate L_∞ and K . We have some fish that were recaptured more than two times so we randomly selected only one pair of recaptures from each to use to estimate the parameters
222 1000 times. We found the mean estimates and mean standard error of those fits, then sampled from within than range to generate a set of von Bertalanffy growth curves to use in our metric uncertainty calculations.

225 We used the full set of marked fish to estimate annual survival ϕ and probability of
recapture p_r using the mark-recapture program MARK implemented in R through
the package **RMark** (Laake, 2013). We fit several models with year, size, and site
228 effects on the probability of survival on a log-odds scale (see full list in Table A4).
For fish that were not recaptured in a particular year, we estimated their size using
our growth model (eqn. 5) and the size recorded or estimated in the previous year.
231 Fish are not well-mixed at our sites and divers needed to swim near an anemone to
have a reasonable chance of capturing the fish on it so we also considered a distance
effect on recapture probability. Using diver GPS tracks, we estimated the minimum
234 distance between a diver and the anemone for each tagged fish in each sample year
to include as a factor. We compared the fit of the models using a modified version of
the Akaike information criterion that reduces the potential for overfitting with small
237 sample sizes (AICc) and selected the model with the lowest AICc value. (Table A4).

Fecundity

We used a size-dependent fecundity relationship determined using photos of egg
240 clutches and females (Yawdoszyn, in prep), where the number of eggs per clutch
(E_c) is exponentially related to the length in cm of the female (L) with size effect
 $\beta_l = 2.388$, intercept $b = 1.174$, and egg age effect $\beta_e = -0.608$ dependent on if the
243 eggs are old enough to have visible eyes. We multiplied the number of eyed eggs per
clutch by the number of clutches per year $c_e = 11.9$ (estimate from Holtswarth et al.,
2017) to get total annual fecundity f of a female of length L :

$$f = c_e * e^{\beta_l \ln(L) + \beta_e [\text{eyed}] + b}. \quad (6)$$

²⁴⁶ **Lifetime egg production**

We used an integral projection model (IPM) (Ellner et al., 2016) with size as the continuous structuring trait z to estimate lifetime egg production (LEP), the expected total number of eggs produced by one recruit. We initialized the IPM with one recruit-sized individual at the initial annual time step ($t = 0$), then projected forward for 100 time steps. We used the size-dependent survival (eqn. B.5) and growth (eqn. 5) functions as the probability density functions in the kernel to describe the survival and growth of the individual into the next time step. We get the size distribution (v_z) at each time step, which represents the probability that the individual has survived and grown into each of the possible size categories, ranging from a minimum of $L_s = 0$ cm to a maximum of $U_s = 15$ cm divided into 100 equal size bins. The probability that the individual is still alive and of any size decreases as the time steps progress; by using a large number of steps, we are able to avoid arbitrarily setting a maximum age and instead let the probabilities become essentially zero.

²⁶¹ We then multiplied the size-distribution v_z at each time by the size-dependent fecundity f_z described above (eqn. 6) to get the total number of eggs produced at each time step. Integrating across time and size gives the total number of eggs one individual is likely to produce in its lifetime:

$$\text{LEP} = \int_{t=0}^{100} \int_{z=L_s}^{z=U_s} v_{z,t} f_z dz dt. \quad (7)$$

When entering the starting individual into the matrix, we use 0.1 as the standard deviation of size to spread the starting individual across size bins. When projecting the distribution of the size of the fish in the next year, we used the size determined by the growth curve (eqn. 5) as the mean along with an estimate of spread to account for differences in fish growth rates. We used our recapture data to estimate the standard deviation (size_{sd}) of the distribution of sizes in the next year of fish starting from one size (A1).

We only considered reproductive effort once the fish has reached the female stage and use the average size of first observation as female for recaptured fish as the transition size $L_f = 9.32\text{cm}$. To incorporate uncertainty, we sampled directly from the sizes at which recaptured fish were first captured as female (5.2 cm - 12.7 cm) (Fig. 3d).

Survival from egg to recruit

We estimate survival from egg to recruit (S_e) using parentage matches to find the number of surviving recruits produced by genotyped parents (similar to the method in Johnson et al., 2018). We scale the number offspring we assign back to parents ($R_m = 62$) by various ways we could have missed offspring in our sampling (P_h , P_c , P_d , and P_s , described below and in Fig. B.1), then divide by the estimated number of eggs produced by genotyped parents (the number of genotyped parents $N_g = 1719$

multiplied by the expected LEP for a fish of parent size LEP_p ;)

$$S_e = \frac{\frac{R_m}{P_h P_c P_d P_s}}{N_g \text{LEP}_p}. \quad (8)$$

We scale the number of matched recruits we find by the cumulative proportion of habitat in our sites we sampled over time ($P_h = 0.41$, details in B.1), the probability of capturing a fish if we sampled its anemone ($P_c = 0.56$, see B.2 for details), and the proportion of the total dispersal kernel area from each of our sites covered within our sampling region ($P_d = 0.28$, calculation in B.3.0.1). Finally, because our dispersal kernel gives the probability of dispersal given that a recruit settled somewhere but our sampling region is not all habitat, we scale by the proportion habitat in our sampling region ($P_s = 0.20$, details in B.3.0.2) to avoid counting this mortality twice.

To estimate local replacement, we scale only by the proportion of habitat we cumulatively sample in our sites and the probability of capturing a fish to estimate the survival and retention of recruits back to our sites: $R_e = \frac{\frac{R_m}{P_h P_c}}{N_g \text{LEP}_p}$.

To incorporate uncertainty in our estimate of egg-recruit survival, we consider uncertainty in the number of offspring assigned to parents during the parentage analysis (R_m) and in the probability of capturing a fish (P_c). We generate a set of values for the number of assigned offspring using a random binomial, where the number of trials is the number of genotyped offspring (745) and the probability of success on each trial is the assignment rate of offspring from the parentage analysis (0.079) (Catalano et al., in prep). For the probability of capturing a fish, we sample values from a beta distribution that captures the mean and variance of capture

probabilities across recapture dives (details in B.2).

Defining recruit and census stage

When assessing persistence, it is important to consider mortality and reproduction that occurs across the entire life cycle to determine whether an individual is replacing itself with an individual that reaches the same life stage (Burgess et al., 2014). We define a recruit to be a juvenile individual that has settled on the reef within the previous year, which also encompasses the size we are first able to sample (3.5-6.0 cm for parentage studies) (Fig. 1). In theory, it does not matter how we define a recruit as long as we use that definition in our calculations of both egg-recruit survival and LEP. In our system, however, while it is straightforward to calculate LEP from any size, we did not have enough tagged recruits to reliably estimate survival to different recruit sizes. Instead, we choose the mean size of offspring matched in the parentage study as our best estimate of the size of a recruit ($\text{size}_{\text{recruit}}$) and test sensitivity to different recruit sizes by sampling from a uniform distribution over the sizes the recruit stage covers (3.5-6 cm, Table A1).

Accounting for density-dependence

Ideally we would assess persistence metrics when the population is at low abundance and not limited by density-dependence. Clownfish have strong social hierarchies and juveniles on an anemone will prevent others from settling there as well (seen in *A. percula*, Buston, 2003a). Each anenome, therefore, can house only one settling clownfish, with anemones already occupied by *A. clarkii* settlers essentially unavail-

able as habitat. This density-dependent mortality will artificially reduce the apparent survival of new recruits, biasing persistence metrics. We account for this density-
 327 dependent mortality by multiplying our estimate of settling recruits (the numerator of eqn. 8) by the proportional increase (DD) in unoccupied anemones at our sites if all of the *A. clarkii* anemones were unoccupied, where p_A is the proportion of
 330 anemones occupied by *A. clarkii* and p_U is the proportion of unoccupied anemones:

$$\text{DD} = \frac{(p_U + p_A)}{p_U} = 1.71.$$
 We present results with this density-dependence modification (with subscript DD: LRP_{DD} in the main text and without in the appendix (Figs.
 333 C.2, C.3)).

Estimated abundance over time

We also consider trends in abundance of breeding females at each site over time ($F_{i,t}$)
 336 to compare to our replacement-based estimates of persistence. Similarly to as we do for offspring, we scale up the number of females caught (F_c) at each site i in each sampling year t by the proportion of habitat sampled in that site and year $P_{h_{i,t}}$ and
 339 by the probability of capturing a fish P_c :

$$F_{i,t} = \frac{F_{c_{i,t}}}{P_{h_{i,t}} P_c} \quad (9)$$

We fit a mixed effects model to estimate the number of fish in each year as a Poisson variable λ_a with site as a random effect m_i using the package `lme4` in R

³⁴² (Bates et al., 2015):

$$\begin{aligned} F_{i,0} &\sim Poisson(\lambda_a) \\ F_{i,t} &= (\lambda_a + m_i)^t. \end{aligned} \tag{10}$$

We estimate λ_a for an average site as well as the individual sites. The population is increasing over time if $\lambda_a > 1$ and decreasing if $\lambda_a < 1$.

(11)

³⁴⁵ Results

From the mark-recapture analysis of tagged and genotyped fish, we estimated mean values of $L_\infty = 10.70$ cm with 95% confidence intervals 9.81-11.65 and $K = 0.864$ ³⁴⁸ (0.80-0.91) for the von Bertalanffy growth curve parameters (eqn. 5, Fig. 3b, Table A1). For juvenile and adult (post-recruitment) survival on a log-odds scale, the best-fit model has an effect of site and a positive effect of size (eqn. B.5, Table A1, Figs. ³⁵¹ 3c, B.3). The accompanying best-fit model for recapture probability has negative effects of size and diver distance from anemone (eqn. B.6, Table A1, Fig. B.4).

For our persistence metrics, we present the estimate using the input values without considering uncertainty (the mean of the uncertainty distributions, with the exception of the size range for recruit), as the best estimate and the range with uncertainty shown in brackets. Using our best estimates for growth, survival, and fecundity, we calculated an average value of LEP across sites of 721 eggs [82, ³⁵⁷ 31132]

(Fig. 4b), with best estimates at individual sites ranging from 0 to 1754 eggs (Fig. C.4). Adult survival has the most effect on the value of LEP (Fig. C.7), with LEP higher the higher the annual survival of adults, who then have more opportunities to reproduce and produce more eggs per clutch when they are larger.

We estimated egg-recruit survival $S_{e_{DD}}$ to be 0.004 [7.5e-05, 0.066] when we correct for density-dependence in our data. Uncertainty in the size of transition to breeding female L_f has the largest effect on egg-recruit survival (Fig. C.9); the larger the transition size to female, the fewer tagged eggs we estimate were produced by our genotyped parents and the higher our estimate of egg-recruit survival. This differs from our finding above that adult survival has the largest effect on LEP because the starting size of the individual considered is lower when we estimate LEP for a recruit (4.37 cm, 3.5-6.0cm range) than LEP for a parent (6.0cm). Fish considered as parents in our parentage analysis have already survived one or more years since recruiting so the transition to breeding female plays a larger role in the number of eggs they are likely to produce than for fish who have just recruited.

We estimated average lifetime recruit production (LRP_{DD}) across sites, the product of LEP_i and $S_{e_{DD}}$, to be 2.89 [0.92, 15.43] (Fig. 4c). Our best estimates of LRP_{DD} at individual sites range from 0 to 7.04 (Fig. C.5). 99.9% of the estimates of LRP with density-dependence compensation and the average best estimate across sites are one or greater, above the threshold necessary for replacement before considering dispersal. This means that individuals at our sites produce enough surviving offspring before considering dispersal to be able to replace themselves, but LRP does not tell us whether those offspring will settle within our sample sites and drive persistence.

381 We did not find any sites with a best estimate of $SP_{DD} \geq 1$ (Fig. 5a), suggesting
that none of our sites could persist in isolation. Though the site Haina ($SP_{DD} =$
384 $0.055 [2.6e-04, 1.27]$) has an SP range that exceeds 1, only 0.1% of the estimates are
 ≥ 1 , making self-persistence very unlikely. We also saw estimates > 1 for Caridad
Cemetery but those were due to the lack of recaptures at that site and the resulting
high uncertainty in adult survival and are unlikely to indicate persistence. I

387 Most of the connectivity occurs among the sites in the northern part of our
sample area, from Palanas to Caridad Cemetery, and at the southern part of our
sample area from Tomakin Dako to Sitio Baybayon (Fig. 5b), where the sites tend
390 to be the largest, have higher abundances, and have higher survivals (though not
entirely). Sites at the edges of our sampling region seem to be the strongest sub-
populations, which means many of the recruits they produce could be exported away
393 from our sites rather than into our sampling region.

For network persistence, our best estimate of the dominant eigenvalue of the
realized connectivity matrix $\lambda_{c_{DD}}$ is 0.31 [0.10, 2.44], $p(\lambda_{c_{DD}} \geq 1) = 0.125$ when we
396 correct for density-dependence in the data (Fig. 5c). Network persistence for our
sites is unlikely but not impossible. Our estimate of local replacement (LR_{DD}) was
0.16 [0.05, 0.88] correcting for density-dependence in the data, also suggesting lack
399 of independent persistence of our group of sites. When we calculated LR using all
arriving recruits to our sites, however, rather than just those originating there, our
best estimate was > 1 (2.08 with 99.8% $\not\sim 1$), suggesting that there is recruit-recruit
402 replacement at our sites when we include immigrant recruits. While both LR_{DD} and
 $\lambda_{c_{DD}}$ tell us about the ability of our sites to persist as an isolated group, they differ

in their assumption of the structure of the population. LR_{DD} gives us the number
405 of recruits individuals at our sites produce that settle within our sites, assuming
the network of sites is a single well-mixed unit, while $\lambda_{c_{DD}}$ accounts for the spatial
structure and multi-generation dynamics.

408 Based on our estimates of LRP_{DD} , LR_{DD} , SP_{DD} , and NP_{DD} , it is possible but
unlikely that our set of sets is able to persist in isolation as a closed system. With
our existing site configuration and dispersal kernel estimate, we would need a value
411 of LRP of 8.84 (an egg-recruit survival of 0.012 with our estimated value of LEP or
a value of LEP of 2203 with our estimated value of $S_{e_{DD}}$) to have a best estimate of
 $\lambda_{c_{DD}} = 1$ and network persistence. Alternately, increasing the amount of habitat in
414 our region (currently about 20%) to 55%, with equally sized and spaced sites with
adult survival of an average site, gives a best estimate of $\lambda_{c_{DD}} = 1$ and suggests
network persistence (Fig. 6a). Considering uncertainty, 95% of the estimates of $\lambda_{c_{DD}}$
417 are > 1 at about 85% habitat (Fig. 6b).

Our estimated abundance of females over time has a slight positive trend for the
average site ($\lambda_a = 1.08$, Fig. 4a), suggesting a slight increase in population size for
420 the population overall through time. Most individual sites also show a slight positive
trend in female abundance through time, though one large site shows declines (Fig.
4a, Fig. C.1s).

423 Discussion

In this first assessment of demographic persistence of a coastal marine metapopula-
tion, we did not find strong evidence for either self-persistence of an individual patch

426 or network persistence of the entire system as an isolated region. Self-persistence of
one of the larger sites or network persistence of the group of sites is possible at the
upper end of our estimates with uncertainty, but neither is suggested by our best
429 estimates or 87.5% of the estimate range. This inability to persist as an isolated
region does not necessarily mean that the populations at our sites are declining,
however. Our assessments of population trends - both abundance over time and
432 replacement of recruits when we include immigrants - find that the population levels
at our sites are stable or increasing slightly. Taken together, our metrics suggest
that the sites in our region have stable populations on average but require input of
435 immigrants to persist. The portion of coastline we sampled is likely a sink region of
a larger metapopulation, given that there does not seem to be a long-term deline in
the population.

438 For our sites to be able to persist as a network on their own, either the number of
surviving recruits produced by an average recruit (LRP) would need to be higher or
more recruits would need to be retained within the region. To see a best estimate of
441 network persistence with our existing site configuration and estimated connectivity,
LRP would be about three times higher than our best estimate, which is within
our range of uncertainty (top 6.9% of estimates) and similar to estimates of lifetime
444 reproductive success that include dispersal to the natal reef in *A. percula* in Kimbe
Bay (Salles et al., 2020), suggesting it is not an unreasonable level of production.
Alternately, higher connectivity and retention of offspring among our sites could
447 lead to network persistence. Though lack of sufficient connectivity and retention is
thought to inhibit network persistence in other systems (e.g., a collection of reserves

for eastern oysters (*Crassostrea virginica*) in the Pamlico Sound in North Carolina; 450 Puckett and Eggleston, 2016), low production of surviving recruits due to poor habitat quality seems the more likely explanation in our system. Our dispersal kernel is comparable to those estimated for other species of reef fish, both similar in shape 453 (e.g., Harrison et al., 2012; DAloia et al., 2015) and with a mean dispersal distance of a similar range to that estimated for *A. percula* in Kimbe Bay (13.3 and 18.9 km compared to our estimate of 8.2 km; Almany et al., 2017), which has been found to 456 be persistent without input from outside reefs (Salles et al., 2015). Our sites have generally low reef health, however, due to anthropogenic effects such as pollution and silt from a nearby gravel mine, which affect habitat and reduce production (as 459 in other clownfish systems; Salles et al., 2020; Hayashi et al., 2019). Adult survival was lower at the two sites just downstream of the gravel mine (N. and S. Magbangon in Fig. B.3).

462 We do not find clear evidence for network persistence for our sites despite estimates of the mean dispersal distance of *A. clarkii* from previous genetic work (11 km, Pinsky et al., 2010) and from our samples (8.2 km, Catalano et al., in prep) 465 that are well within the 30 km span of our sites. Though the length of our sampling region is more than twice the mean dispersal distance, usually sufficient for persistence of a population in an isolated reserve (e.g. Lockwood et al., 2002), our 468 sampling region contains only about 20% habitat, rather than a continuous stretch, which may be too low of habitat coverage to support network persistence. Our sensitivity test to proportion habitat suggests that about 2.75 times more habitat in our 471 sampling region would give a best estimate with network persistence, with 50% of

our estimates showing persistence ($\lambda_{C_{DD}} \geq 1$) at about 30% habitat. Our individual sites are likely too small to see self-persistence: the largest site, Haina, is only about
474 0.8km wide, about 10 times smaller than the mean dispersal distance. This is in contrast to the findings on reefs surrounding the isolated Kimbe Island, where the overall population of *A. percula* and several lagoon subpopulations of similar size
477 as our sites were self-persistent (Salles et al., 2015). Our sites are in an area that was hit in 2013 by Typhoon Haiyan, one of the strongest typhoons ever to make landfall, so reef habitat has recently been destroyed in the area, including one of our
480 northern sampling sites. The suggestion of a habitat shortage in our sampling region is partially dependent on our assumption that larvae land in non-habitat between patches and die. Larvae have some navigational and habitat-finding capabilities (e.g.
483 Elliott et al., 1995; Fisher, 2005), so we could be underestimating their ability to find habitat in our calculations, which would decrease the amount of habitat required for network persistence.

486 We suggest that our region is a sink area of a larger metapopulation but the area required for the larger persistent metapopulation depends on the production and connectivity of outside patches. If surrounding patch populations have a similar
489 LRP and level of connectivity as our sites, increasing the area of the network to include them also would not achieve network persistence. If nearby sites have higher egg production or egg-recruit survival, however, it might not take much of an increase
492 in area considered to create a persistent network. Nearby reef sites such as Cuatro Islas, with higher coral cover and less silt, could have higher survival of fish and be contributing recruits to our sites.

495 An alternative to our sampled sites as a sink portion of a larger metapopulation
is that variability in demography or dispersal on a longer scale than our sampling
time could lead to persistence. For example, rockfish on the west coast of the United
498 States have highly variable and episodic recruitment, where successful recruitment
events occur on the decadal scale and sustain the population until the next strong
recruitment event (e.g., Tolimieri and Levin, 2005). Though perhaps not as extreme
501 as in the California Current system, ocean connectivity is still variable in the Coral
Triangle region surrounding our study sites, with estimates suggesting that 20 year
simulations are necessary to capture the full extent (Thompson et al., 2018). Our
504 study, though relatively long term, could have missed a particularly strong recruit-
ment event that would enable local persistence of the set of populations we sampled.

Though we estimate abundance trends and do not find overall declines, it is
507 possible we could have missed declines due to our sampling design. Our sampling
study was designed for mark-recapture analyses rather than a comprehensive habitat
or abundance estimate so we did not sample all areas of all sites each year. We scale
510 up the number of fish we caught to account for those we missed using the proportion
of metal-tagged anemones we visited, which assumes that all tagged anemones are
equally likely to be sampled. In reality, tags that no longer have anemones next to
513 them are likely harder to find and sample. If anemones are disappearing over time
at our sites, we might be overestimating the number of fish present and missing that
our site are declining and not persistent even with outside input.

516 NEED TO EDIT THIS UNCERTAINTY PARAGRAPH! Including uncertainty
in our empirical estimates of demographic and dispersal parameters allows us to

better understand how likely it is that the population is persistent and which processes contribute the most uncertainty. We see a wide range of estimated metric values, spanning of network persistence for our set of sites to far from it. In our study, demographic parameters, particularly adult survival, also have a large effect on whether or not we think the population is persistent. Other metapopulation studies also find higher sensitivity to demographic rather than connectivity parameters (e.g., on source or sink status in bicolor damselfish; Figueira, 2009), including particular sensitivity to adult survival (on metapopulation growth rate in mussels; Carson et al., 2011). Our estimates of connectivity are simpler than our estimates of demography, with no spatial variability (which can be important in understanding demographic connectivity; Johnson et al., 2018), and a more thorough assessment could alter their relative effect on persistence, but this suggests that sufficient offspring production and survival has a larger effect on persistence at these relatively small scales of connectivity. Uncertainty in our sampling, particularly how likely we are to capture a fish, however, contributes the most uncertainty to whether we determine the population to be persistent, highlighting the challenge of estimating these metrics empirically. For a marine metapopulation, our system is relatively uncomplicated; as we accumulate more empirical assessments of metapopulations to compare to our expectations from theory and models, we will have to think carefully about how to handle uncertainty as we move to tackling larger and more complicated systems.

Persistence criteria, such as those detailed in Hastings and Botsford (2006) and Burgess et al. (2014), ask whether a population at low abundance can grow and

recover rather than going extinct. Density-dependence is often ignored at low abundances (Botsford et al., 2019) so is not explicitly considered in persistence metrics.

543 In real populations, however, it can be challenging to estimate density-independent demographic rates, as density-dependence is occurring in the population as it is sampled. In *A. clarkii*, density-dependence is likely most important immediately

546 post-settlement, as for many fish species, but is also relatively easy to measure at that point and accounted for in our analyses. Density-dependence could continue to be important throughout the life history, however, due to the social hierarchies

549 in colonies of clownfish (e.g. Buston and Elith, 2011). In other species of clownfish, individuals on the same anemone maintain strict size spacing, restricting their food intake and growth to avoid encroaching on the position of another fish and being

552 attacked or evicted (seen in *A. percula*, Buston, 2003a,b). This suggests that while fish are in the pre-reproductive queue, density-dependence may lower growth rates compared to the growth of fish alone on an anemone, as would be the case in a pop-

555 ulation at low abundance. We include the primary effect of density-dependence on our estimate of egg-recruit survival but other estimates, particularly growth and sur-

vival, would also likely be higher in the absence of density-dependence and increase

558 LRP.

Understanding persistence is critical for management of spatial-structured populations, such as siting marine protected areas XX, assessing habitat fragmentation

561 risks, and conserving species in the face of climate change XX. Though models and theory provide us with expectations, we are only recently beginning to be able to tackle these questions of persistence empirically in model systems such as clownfish

564 and other sedentary tropical reef fish (e.g., Salles et al., 2015; Johnson et al., 2018).
With parentage analyses now being extended to temperate species (e.g., Baetscher
et al., 2019) and better understanding of how biophysical models compare to lar-
567 val dispersal patterns (Bode et al., 2019) we are beginning to move beyond model
species and investigate persistence in harvested and spatially-managed systems (e.g.,
Garavelli et al., 2018). Our study shows the importance of long term sampling and
570 careful consideration of the different demographic processes that affect our metric
calculations, such as density-dependence and sampling biases, to understand marine
population dynamics in empirical systems.

573 **Figures**

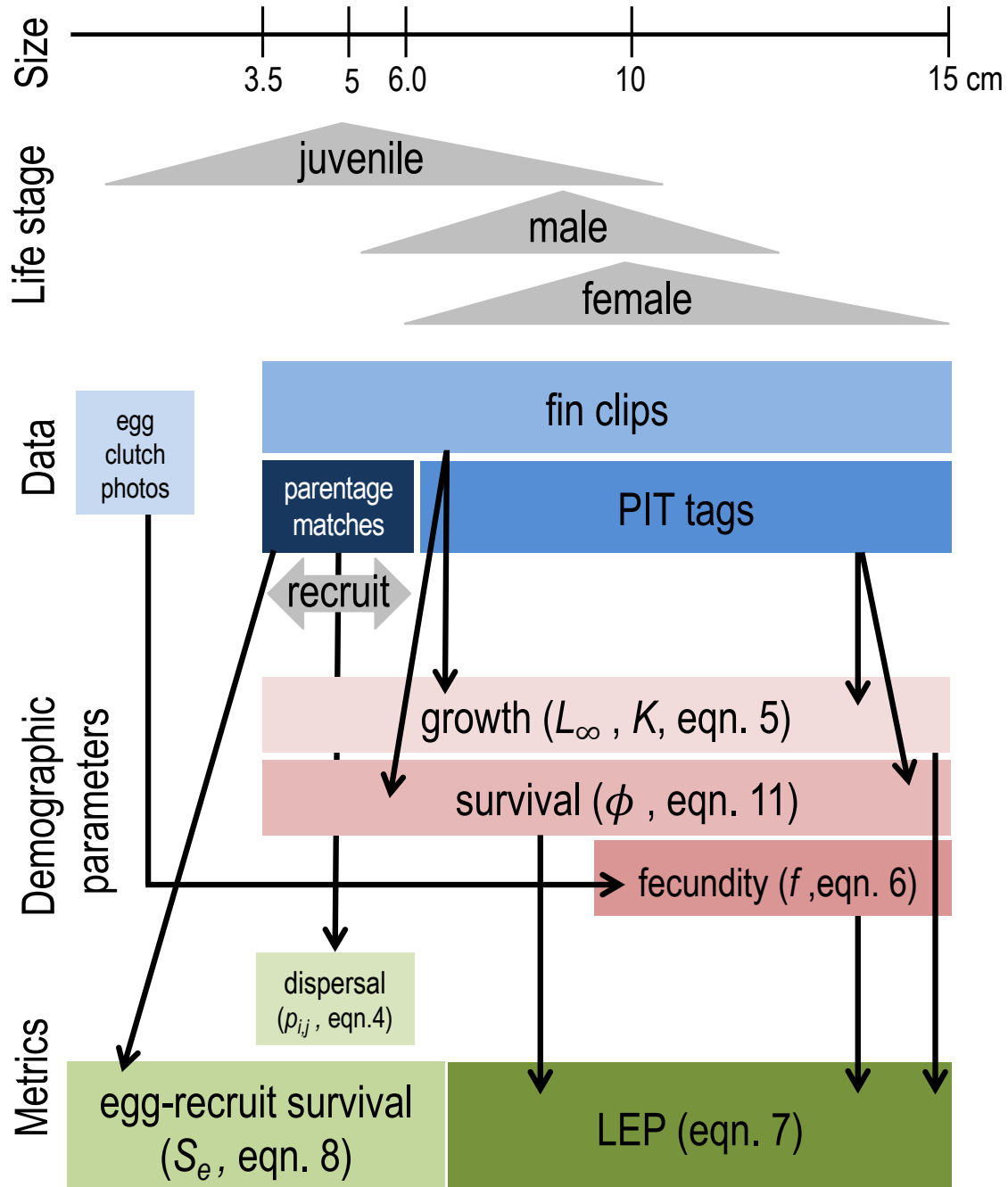


Figure 1: The data collected for fish at each life stage and how they match to the equations and metrics estimated. We consider recruits to be offspring in their first year of settlement, represented by the 3.5-6.0 cm range.

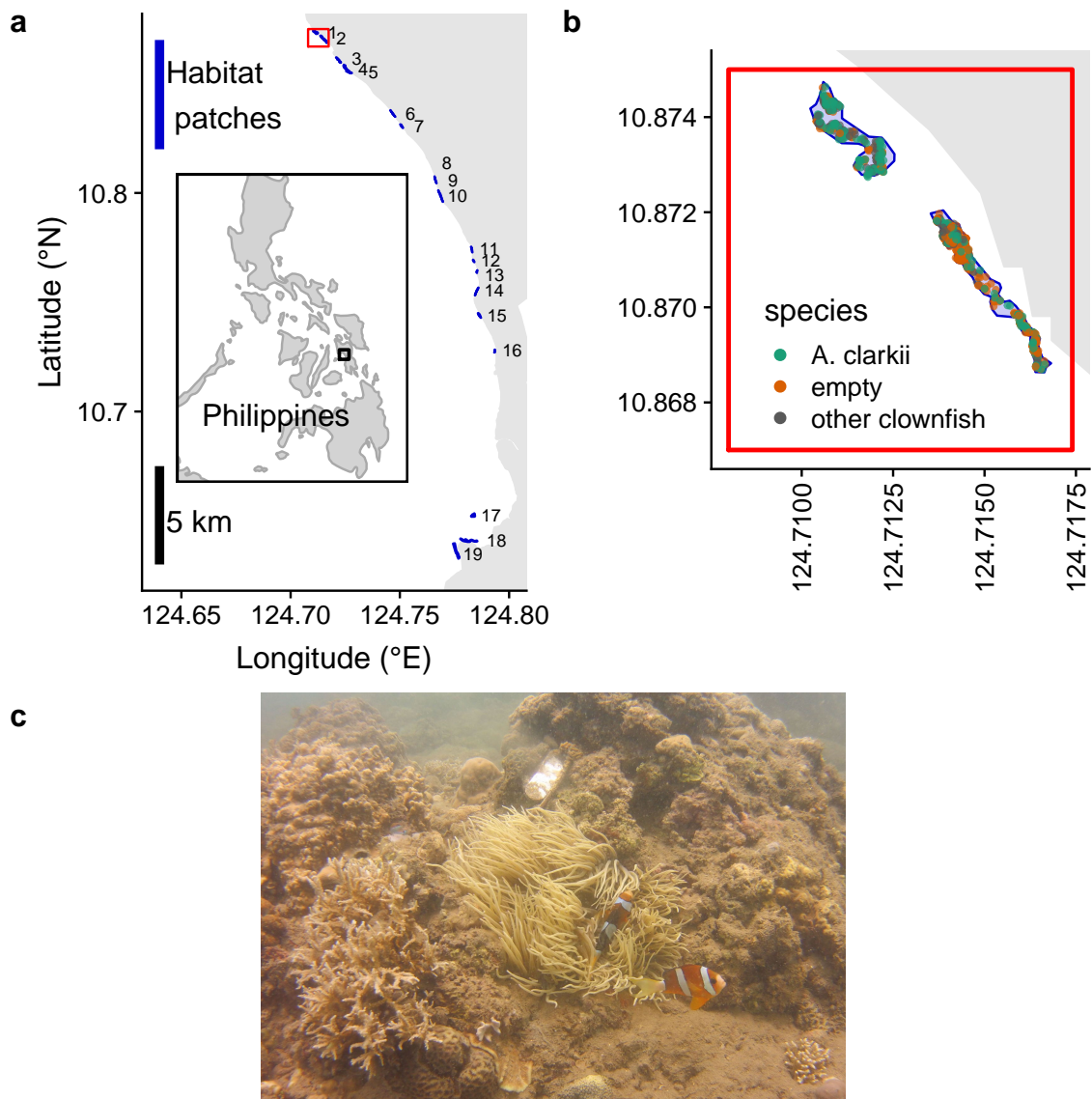


Figure 2: a) Map of the sites along the coast of Leyte in the Philippines. From north to south, the patches are: 1) Palanas, 2) Wangag, 3), North Magbangon, 4) South Magbangon, 5) Cabatoan, 6) Caridad Cemetery, 7) Caridad Proper, 8) Hicop South, 9) Sitio Tugas, 10) Elementary School, 11) Sitio Lonas, 12) San Agustin, 13) Poroc San Flower, 14) Poroc Rose, 15) Visca, 16) Gabas, 17) Tomakin Dako, 18) Haina, and 19) Sitio Baybayon. b) Zoomed-in map of the two northern-most sites, Palanas and Wangag, to show anemone arrangement with anemones colored as occupied by *A. clarkii* (green), occupied by other clownfish species (orange), or unoccupied by clownfish (grey). c) An example anemone occupied by *A. clarkii* in a typical habitat at the sites. The metal anemone tag is visible just above the anemone on the rock.

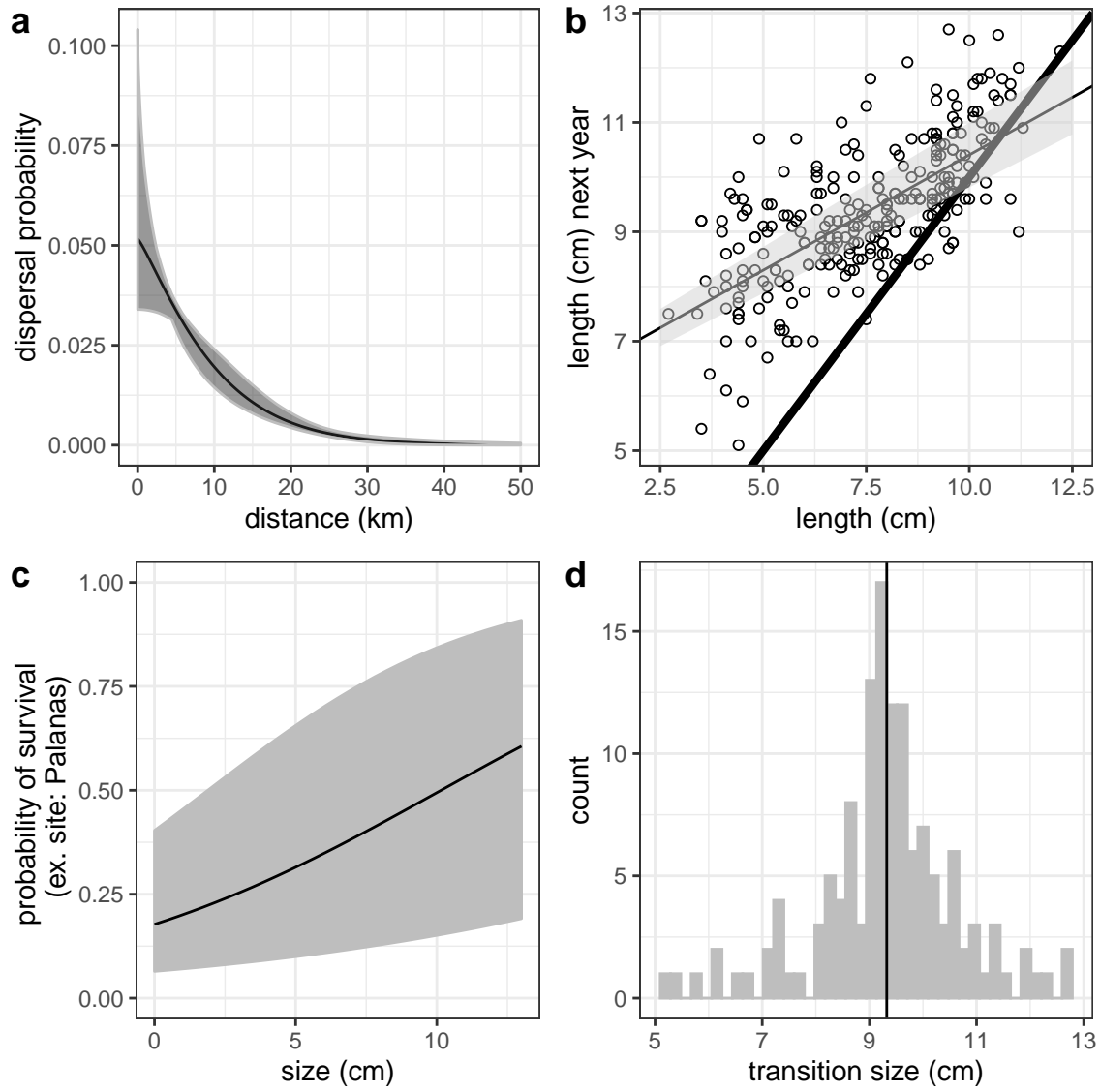


Figure 3: Best estimates (solid black line) and uncertainty (grey) for dispersal (a), growth, including the 1:1 line in thick black (b), post-recruit annual survival at Palanas as an example site (c), and size at female transition (d) parameters. Best est

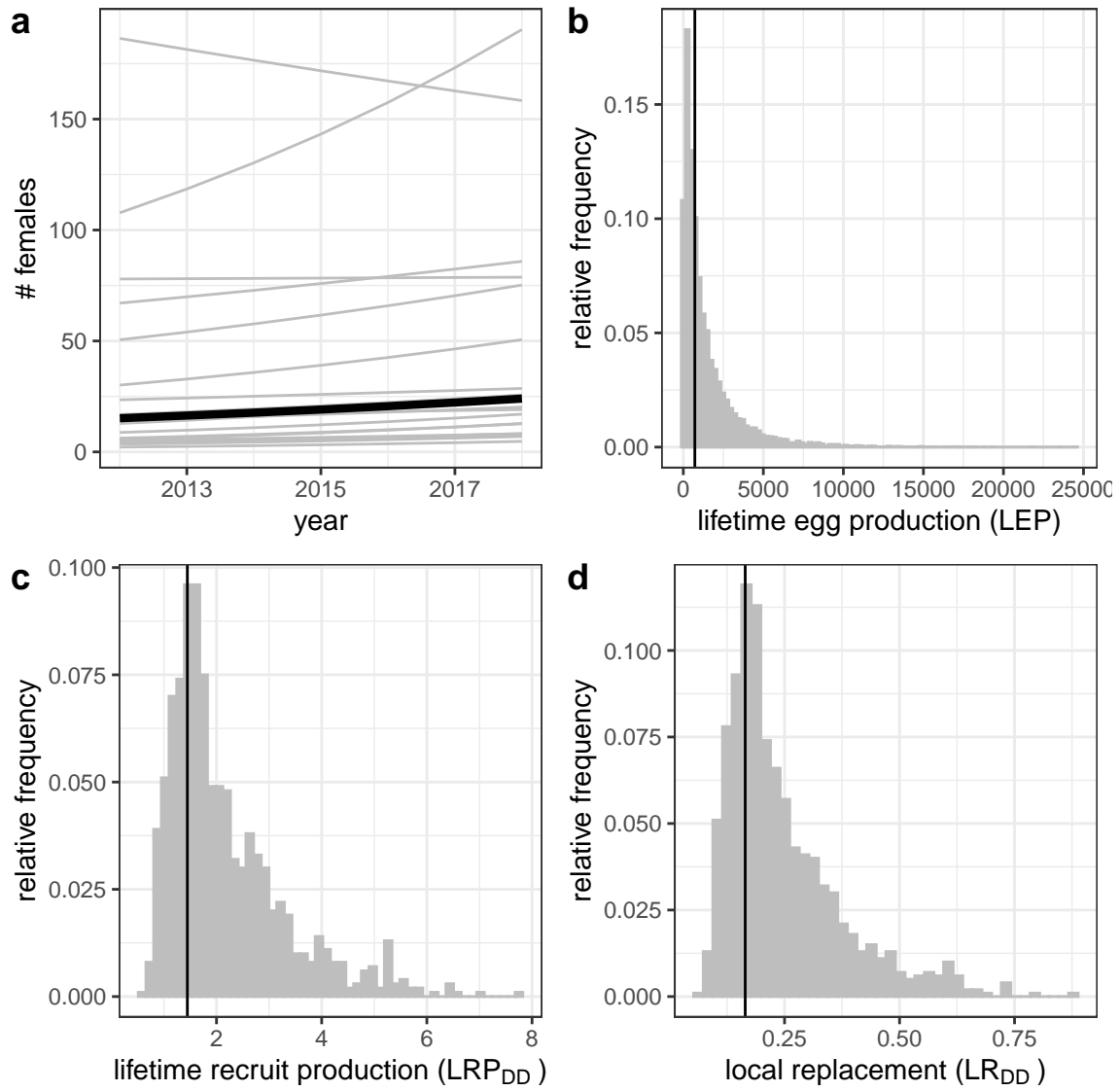


Figure 4: Estimates of a) estimated abundance of females over time at each individual site (grey lines) and for an average site (black line), b) individual-site LEP for all sites with the best estimate averaged across sites (black line), c) average LR_{DD} across sites, and d) local replacement, showing the best estimate (black solid line) and range of estimates considering uncertainty in the inputs (grey). Estimates of LRP and local replacement include compensation for density-dependent mortality in early life stages.

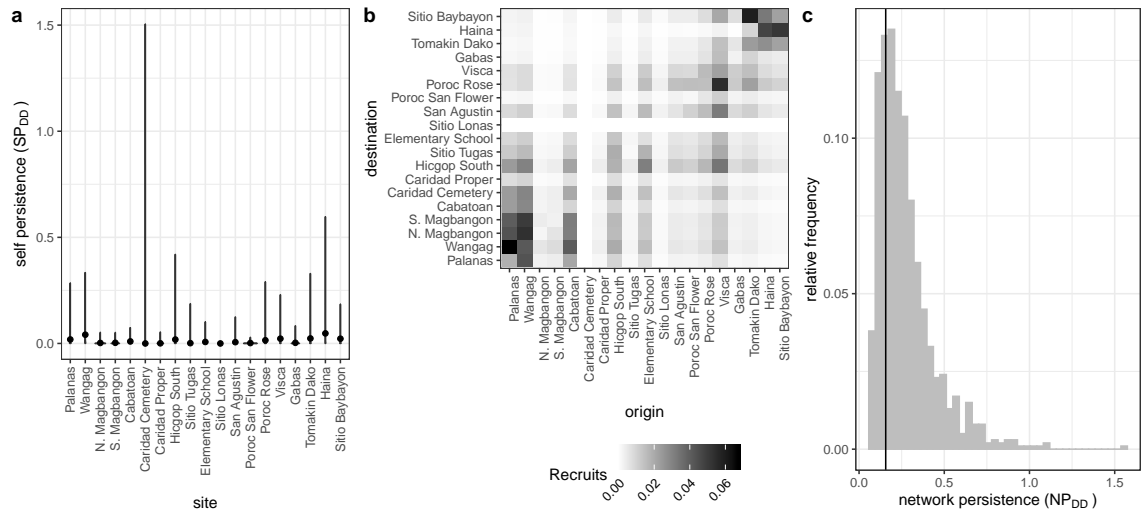


Figure 5: Values of self-persistence (a), realized connectivity among sites (b), and network persistence (c). All estimates include compensation for density-dependence in early life stages. For self-persistence (a) and network persistence (c), the best estimate is shown with in black (point for (a), line for (c)) and the range of estimates considering uncertainty is shown in grey.

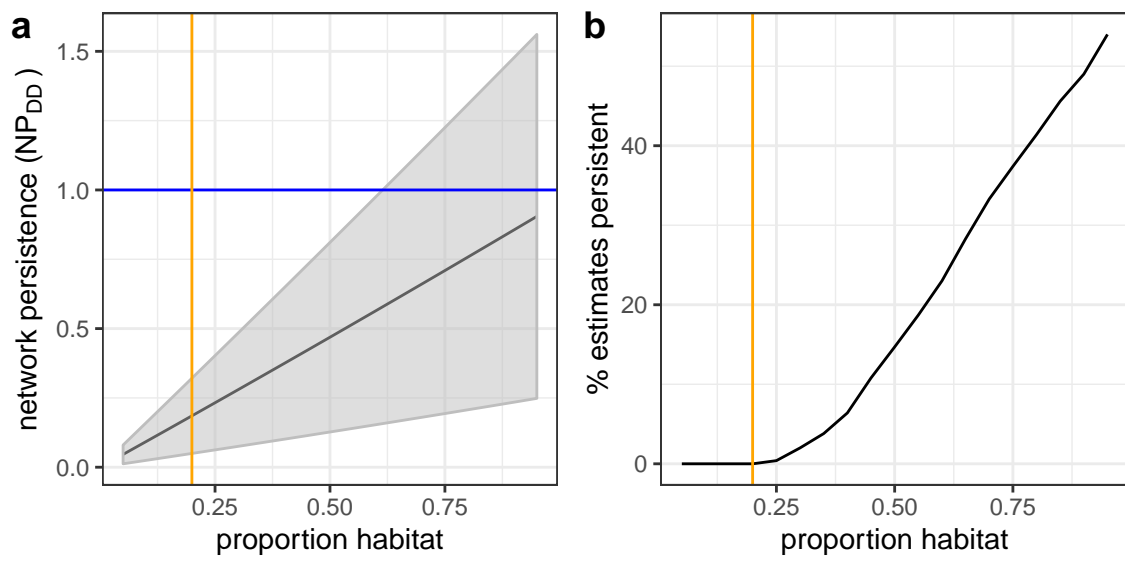


Figure 6: Sensitivity of network persistence to the proportion of the sampling region that is habitat. (a) The best estimate of λ_{cDD} with the standard deviation of the estimates with uncertainty for 19 patches of equal size and spacing with adult survivals for an average patch. (b) The percentage of estimates from the runs in (a) with $\lambda_{cDD} \geq 1$ with increasing proportion habitat.

Appendix

A Summary of parameters

Parameter	Description	Best estimate	Range in uncertainty runs	Notes
k_d	scale parameter in dispersal kernel	-2.33	-2.81 to -1.22	eqn. 4, estimated using methods in Bode et al. (2018) in Catalano et al. (in prep)
θ	shape parameter in dispersal kernel	1.19	0.63 to 2.04	eqn. 4, estimated using methods in Bode et al. (2018) in Catalano et al. (in prep)
L_∞	average asymptotic size (cm) in von Bertalanffy growth curve	10.70 cm	9.81 to 11.65 cm	eqn. 5
K	growth coefficient in von Bertalanffy growth curve	0.864	0.80 to 0.91	eqn. 5

$b_{\phi_{Cabatoan}}$	intercept for adult survival at 0 cm at Cabatoan	-1.78	± 0.33 standard error	on a log-odds scale, eqn. B.5
$i_{\phi_{Cardidad Cemetery}}$	addition to intercept for survival at Caridad Cemetery	-19.61	± 2994 standard error	on a log-odds scale, eqn. B.5
$i_{\phi_{Elementary School}}$	addition to intercept for survival at Elementary School	-0.11	± 0.41 standard error	on a log-odds scale, eqn. B.5
$i_{\phi_{Gabas}}$	addition to intercept for survival at Gabas	-0.42	± 0.58 standard error	on a log-odds scale, eqn. B.5
$i_{\phi_{Haina}}$	addition to intercept for survival at Haina	0.12	± 0.35 standard error	on a log-odds scale, eqn. B.5
$i_{\phi_{Hicgop South}}$	addition to intercept for survival at Hicgop South	-0.06	± 0.46 standard error	on a log-odds scale, eqn. B.5

$i_{\phi_{N.Magbangon}}$	addition to intercept for survival at N. Magbangon	-1.31	\pm 0.38 standard error	on a log-odds scale, eqn. B.5
$i_{\phi_{Palanas}}$	addition to intercept for survival at Palanas	0.24	\pm 0.26 standard error	on a log-odds scale, eqn. B.5
$i_{\phi_{PorocRose}}$	addition to intercept for survival at Poroc Rose	-0.19	\pm 0.44 standard error	on a log-odds scale, eqn. B.5
$i_{\phi_{PorocSanFlower}}$	addition to intercept for survival at Poroc San Flower	-0.52	\pm 0.48 standard error	on a log-odds scale, eqn. B.5
$i_{\phi_{SanAgustin}}$	addition to intercept for survival at San Agustin	-0.47	\pm 0.50 standard error	on a log-odds scale, eqn. B.5
$i_{\phi_{SitioBaybayon}}$	addition to intercept for survival at Sitio Baybayon	0.02	\pm 0.26 standard error	on a log-odds scale, eqn. B.5

$i_{\phi_{S.Magbangon}}$	addition to intercept for survival at S. Magbangon	-1.08	\pm 0.48 standard error	on a log-odds scale, eqn. B.5
$i_{\phi_{TomakinDako}}$	addition to intercept for survival at Tomakin Dako	0.39	\pm 0.33 standard error	on a log-odds scale, eqn. B.5
$i_{\phi_{Visca}}$	addition to intercept for survival at Visca	0.33	\pm 0.35 standard error	on a log-odds scale, eqn. B.5
$i_{\phi_{Wangag}}$	addition to intercept for survival at Wangag	0.35	\pm 0.25 standard error	on a log-odds scale, eqn. B.5
b_a	size effect for adult survival	0.15	\pm 0.03 standard error	on a log-odds scale, eqn. B.5
β_e	coefficient for eyed eggs	-0.608		eqn. 6, Yawdoszyn et al. (in prep)
β_l	size effect in eggs-per-clutch relationship	2.39		eqn. 6, Yawdoszyn et al. (in prep)

b	intercept in eggs-per-clutch relationship at female size 0 cm	1.17		eqn. 6, Yawdoszyn et al. (in prep)
c_e	egg clutches per year	11.9		eqn. 6, Holtswarth et al. (2017)
$\text{size}_{\text{recruit}}$	size (cm) of recruited offspring	mean of size of offspring in parentage analysis = 4.37 cm	3.5 - 6.0 cm	drawn from uniform distribution across range
$\text{size}_{\text{recruit},sd}$	standard deviation of size of a recruit	0.1		used in discretization of IPM for LEP
size_{sd}	standard deviation distribution of sizes of a fish in the next year	1.45		used in discretization of IPM for LEP, estimated from range of sizes for fish starting at 7.4-7.6 cm and recaptured a year later

L_s	minimum size in LEP IPM	0 cm		eqn. 7
U_s	maximum size in LEP IPM	15 cm		eqn. 7
L_f	size at transition to female	9.32 cm	5.2 - 12.7 cm	drawn from distribu- tion in data
R_m	number of off- spring matched to parents	62 offspring		eqn. 8
N_g	number of geno- typed parents	1719 fish		eqn. 8
P_h	proportion of sites sampled cumulatively across time	0.41		eqn. 8, details in B.1
P_d	proportion of dispersal kernel area from each site covered by our sampling region	0.28		eqn. 8, details in B.3.0.1

P_c	probability of capturing a fish	0.56	drawn from beta distribution with parameters $\alpha_{P_c} = 1.44$ and $\beta_{P_c} = 1.13$	eqn. 8, details in B.2
P_s	proportion of our sampling region that is habitat	0.20		eqn. 8, details in B.3.0.2
DD	proportion of habitat that would be available without density-dependence at settlement	1.71		eqn. 8
p_U	proportion of anemones unoccupied by clownfish	0.53		used to estimate DD

p_A	proportion of anemones occupied by $A.$ <i>clarkii</i>	0.38		used to estimate DD
-------	--	------	--	---------------------

Table A1: Summary of parameter symbols, definitions, and values.

⁵⁷⁶ **B Method details**

B.1 Proportion of habitat sampled

We used tagged anemones to estimate the proportion of habitat sampled at each site in each year ($P_{h_{i,t}}$). We tagged each anemone that is home to $A.$ *clarkii*, with a metal tag, which is relatively permanent and easy to re-sight (the anemone tag is visible above the anemone in Fig. 2c), so we consider the total number of metal tags at each site to be the total number of anemones that are habitat. We divide the number of tagged anemones visited each sampling year by the total number of metal tags at that site to get the proportion of habitat sampled. We use proportion of anemones rather than proportion of total site area because anemones, and therefore habitat quality, are unevenly distributed across the site; areas we did not visit are likely to have a lower density of anemones than the areas we did sample.

⁵⁸⁸ For scaling the number of tagged recruited offspring to account for areas of our sites we did not sample, we use the overall proportion habitat sampled across all sites and sampling years (P_h). We sum the metal-tagged anemones we visited across all

Site	# Total anems	% Habitat surveyed						
		2012	2013	2014	2015	2016	2017	2018
Cabatoan	26	42	58	58	65	73	0	62
Caridad Cemetery	4	0	75	50	0	50	50	50
Elementary School	8	0	100	38	88	88	88	100
Gabas	9	0	0	0	44	44	67	0
Haina	104	0	6	13	13	10	56	80
Hicgop South	18	0	67	22	28	56	83	78
N. Magbangon	105	5	12	40	63	63	0	5
S. Magbangon	34	41	56	32	0	65	0	71
Palanas	137	29	58	47	63	85	86	86
Poroc Rose	13	100	100	69	31	23	69	69
Poroc San Flower	11	100	82	73	73	55	82	64
San Agustin	17	94	65	71	65	100	82	76
Sitio Baybaon	260	0	14	30	33	30	41	80
Tomakin Dako	50	0	24	22	36	34	60	68
Visca	13	100	100	23	38	62	85	62
Wangag	296	18	32	42	34	26	49	68

Table A2: Table showing the percent of metal-tagged anemones surveyed at each site in each sampling year.

591 sites and years to get the total number of metal-tagged anemones we visited while
 sampling. We then divide that by the number of anemones we could have sampled,
 the sum of total metal-tagged anemones across all sites multiplied by the number of
 594 sampling years, to get the overall proportion habitat sampled across our sites and
 sampling years.

B.2 Probability of capturing a fish, from recapture dives

597 We use mark-recapture data from recapture dives done within a sampling season
to estimate the probability of capturing a fish. During some of the sampling years,
portions of the sites were sampled again within a few weeks of the original sampling
dives. We assume there is no mortality of tagged fish between the original sampling
dives and the recapture dives because they are so close in time and that fish do not
change their behavior or response to divers, so therefore assume that the probability of
603 recapturing a fish is the same as the probability of capturing a fish on a sampling dive.
For each recapture dive, we use GPS tracks of the divers to identify the anemones
covered in the recapture dive and the set of PIT-tagged fish encountered on those
606 anemones during the original sampling dives. We estimate the probability of capture
 P_c as the number of tagged fish caught during the capture dive m_2 divided by the
total number of fish caught on the recapture dive n_2 : $P_c = \frac{m_2}{n_2}$. The value of P_c from
609 each recapture dive is reported in Table A3.

We use the mean P_c across all 14 recapture dives, covering XX sites in 3 sampling
seasons (2016, 2017, 2018), as our best estimate. Because there are so few recapture
612 dives compared to the number of times we calculate the metrics to show the range
of uncertainty, we represent the probability of capture as a distribution, rather than
sampling directly from the values calculated for each recapture dive. The distribution
615 of capture probabilities across the 14 dives is quite skewed so we represent it as a
beta distribution, using the mean μ_{P_c} and variance V_{P_c} of the set of 14 values to find
the appropriate α_{P_c} and β_{P_c} parameters, where

$$\alpha_{P_c} = \left(\frac{1 - \mu_{P_c}}{V_{P_c}} - \frac{1}{\mu_{P_c}} \right) \mu_{P_c}^2 \quad (\text{B.1})$$

$$\beta_{P_c} = \alpha_{\mu_{P_c}} \times \frac{1}{\mu_{P_c} - 1}. \quad (\text{B.2})$$

618 The mean of the individual capture probability values is $\mu_{P_c} = 0.56$, with variance
 $V_{P_c} = 0.069$, which gives beta distribution parameters $\alpha_{P_c} = 1.44$ and $\beta_{P_c} = 1.13$. We
sample 1000 values from the beta distribution, then truncate the sample to only val-
621 ues larger than the lowest value of P_c estimated in an individual dive (0.20), to avoid
extremely low values that are sometimes randomly sampled from the distribution
but are unrealistically low. We then sample with replacement from the truncated
624 set to get a vector of values the length of the number of runs.

Talk to Katrina to fill out table with data that went into recapture calcs

Site	Year	m_2	n_2	P_c
				0.56
				0.26
				0.89
				0.67
				0.20
				0.83
				0.47
				0.20
				0.83
				1.0
				0.33
				0.58
				0.63
				0.41

Table A3: Table showing the site, year, number of fish caught on sample dives on the anemones resampled during the recapture dive (m_2), number of fish caught on the recapture dive (n_2) for each recapture dive.

B.3 Scaling up recruits

627 To estimate the total number of offspring produced by our genotyped parents that
survive to recruitment, we scale up the number of matched offspring caught during
sampling (R_m) to account for recruits we could have missed (Fig. B.1). We scale
630 up by 1) the cumulative proportion of habitat we sampled at our sites over time
(P_h) to account for recruits at anemones we did not sample (details in B.1), 2) the
probability of capturing a fish if we sampled its anemone (P_c) to account for fish that
633 escaped during sampling (details in B.2), 3) the proportion of the dispersal kernel
from our sites within of our sampling region (P_d) to account for fish that dispersed
outside of our sampling area (details in B.3.0.1), and 4) the proportion habitat in our

636 sampling region (P_s) to avoid counting mortality of fish dispersing to non-habitat
 within our region twice (in both the estimate of total recruits and in the integrated
 dispersal kernel) (details in B.3.0.2), and 5) the proportion of anemones occupied by
 639 *A. clarkii* (DD) to account for density-dependent mortality of settling recruits.

How could we have missed potential recruits originating from our sites?

- 1) Failed to catch recruit when sampling (P_c)
- 2) Missed sampling some habitat areas within our sites (P_h)
- 3) Recruit dispersed outside our study region (P_d)
- 4) Recruit dispersed to non-habitat within our region (P_s)
- 5) Recruit died due to density-dependent competition with other settlers (DD)

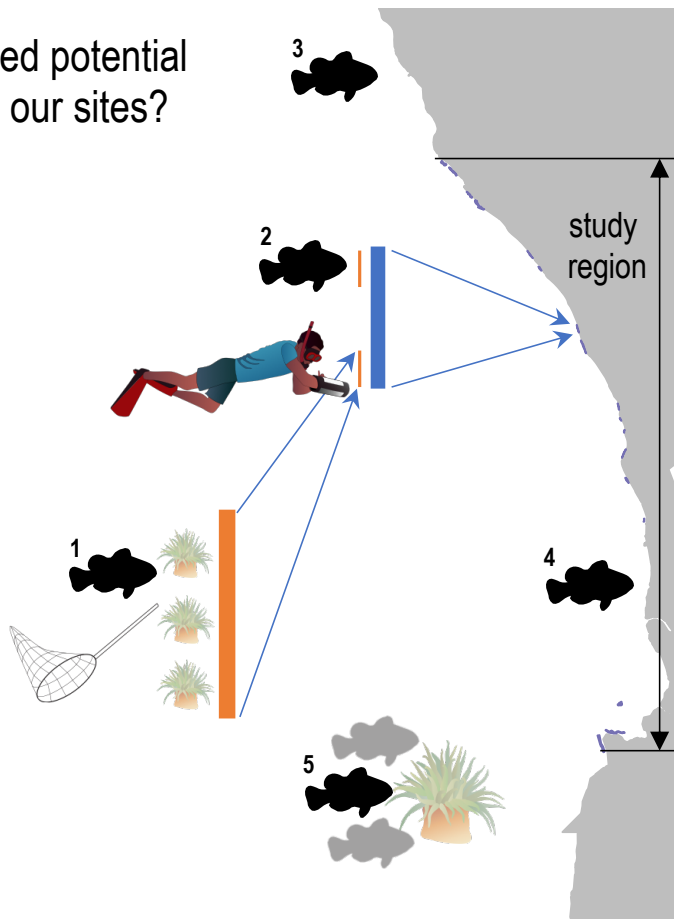


Figure B.1: Schematic of five ways we could have missed recruits while sampling and used to scale up our raw estimate of recruits from matched offspring.

B.3.0.1 Proportion of dispersal kernel area sampled

To account for recruits that dispersed outside our sampling region, we find the proportion of the dispersal kernels from all parents that falls within our sampling region.
 642 For each of the nineteen sites, we find the area (A_i) under the kernel from the center of the site to the north edge of the sampling area (d_N) (northern-most tagged
 645 anemone at Palanas, the northern-most site) and the center of the site to the south edge of the sampling area (d_S) (southern-most tagged anemone at Sitio Baybayon, the southern-most site), then multiply by the number of genotyped parents at that
 648 site (N_{g_i}). We add the total areas together, then divide by the sum of the total area under the dispersal kernel in both directions (1 when kernel is normalized to 0.5) multiplied by the total number of genotyped parents (N_g) to get the proportion of
 651 the total dispersal kernel area covered by our sampling region (P_d):

$$A_i(d) = N_{g_i} \int_0^{d_N} z e^{-(zd)^{\theta}} dd, \quad (\text{B.3})$$

$$P_d = \frac{\sum_{i=1}^{19} A_i}{N_g}. \quad (\text{B.4})$$

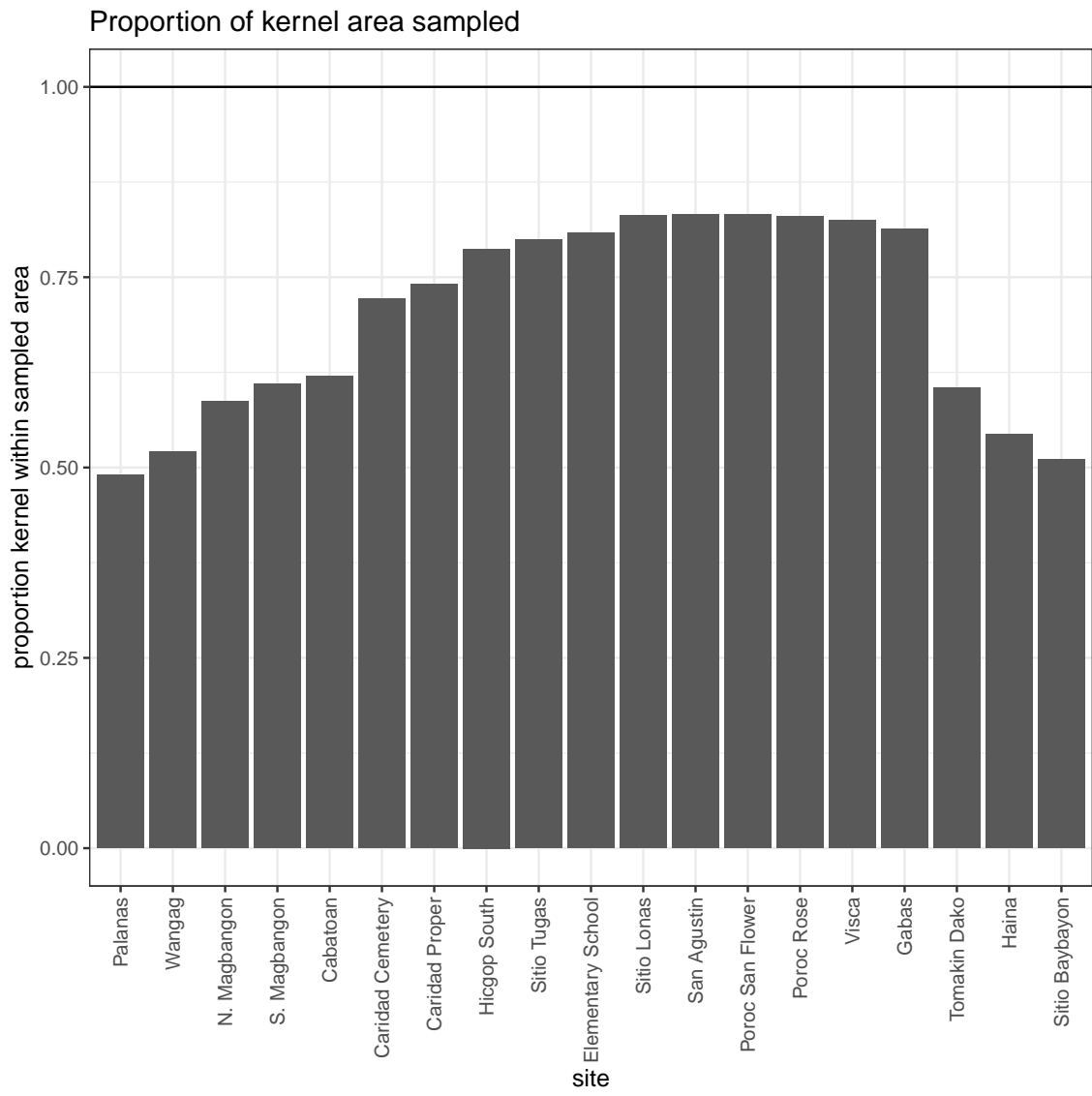


Figure B.2: Proportion of the dispersal kernel area from the center of each site covered by our sampling. Our overall proportion is weighted by the number of parents at each site.

B.3.0.2 Proportion habitat in sampling area

We assume that larvae are unable to navigate to habitat if they attempt to settle
654 on an unsuitable patch, though clownfish larvae do likely have some ability both to
sense good settlement areas, either by detecting host anemones (Elliott et al., 1995;
Arvedlund et al., 1999) or conspecifics (e.g. Lecchini et al., 2005, for coral reef fish
657 more broadly), and swim in particular direction (e.g. Bellwood and Fisher, 2001;
Fisher, 2005). To avoid counting mortality due to settling on non-habitat twice -
once in scaling up our matched recruits, which only includes those who settled on
660 habitat, and once in integrating the dispersal kernel, we scale our estimate of total
surviving recruits from our patches by the proportion of our sampling region that
is habitat (P_s). We find P_s by summing the lengths of all of our sites, which run
663 approximately north-south, and dividing that by the total distance north-south of
our sampling region, giving $P_s = 0.20$.

Model	Model description	AICc	dAICc
$\phi \sim S, p \sim S + D$	survival size, recapture size+distance	3348.861	0
$\phi \sim S, p \sim D$	survival size, recapture distance	3359.998	-11.1371
$\phi, p \sim D$	survival constant, recapture distance	3383.175	34.3141
$\phi, p \sim S + D$	survival constant, recapture size+distance	3384.959	36.0981
$\phi \sim t, p$	survival time, recapture constant	3408.342	59.4816
$\phi \sim i, p$	survival site, recapture constant	3440.842	91.98112
$\phi \sim i, p \sim S + D$	survival site, recapture size+distance	3440.842	91.98112
$\phi, p \sim t$	survival constant, recapture time	3453.609	104.74839
$\phi \sim S, p \sim S$	survival size, recapture size	3527.710	178.84940
ϕ, p	survival constant, recapture constant	3570.908	222.04690

Table A4

B.4 Full set of MARK models

666 We consider the following set of models in MARK for survival (ϕ) and recapture (p) probability, including effects of size (S), minimum distance from diver to anemone during surveys (D), time (t), and site (i) (Table A4):

669 The best model for post-recruitment annual survival ϕ has a positive size effect
 (670 $b_a = 0.169 \pm 0.028$ SE UPDATE THESE NUMBERS!) with intercepts varying by site (eqn. B.5, Fig. B.3). The best model for recapture probability p_r has a negative effect of size (671 $b_1 = -1.816 \pm 0.080$ SE UPDATE THESE NUMBERS!) and a negative effect of diver distance from anemone (672 $b_2 = -0.171 \pm 0.021$ SE UPDATE THESE NUMBERS!), with intercept $b_{p_r} = 17.93 \pm 0.858$ SE UPDATE THESE NUMBERS! (eqn. B.6, Fig. B.4), suggesting divers are less likely to recapture larger fish and those

at anemones far from areas sampled.

$$\log\left(\frac{\phi}{1-\phi}\right) = b_{\phi_i} + b_a \text{size}. \quad (\text{B.5})$$

$$\log\left(\frac{p_r}{1-p_r}\right) = b_{p_r} + b_1 \text{size} + b_2 d. \quad (\text{B.6})$$

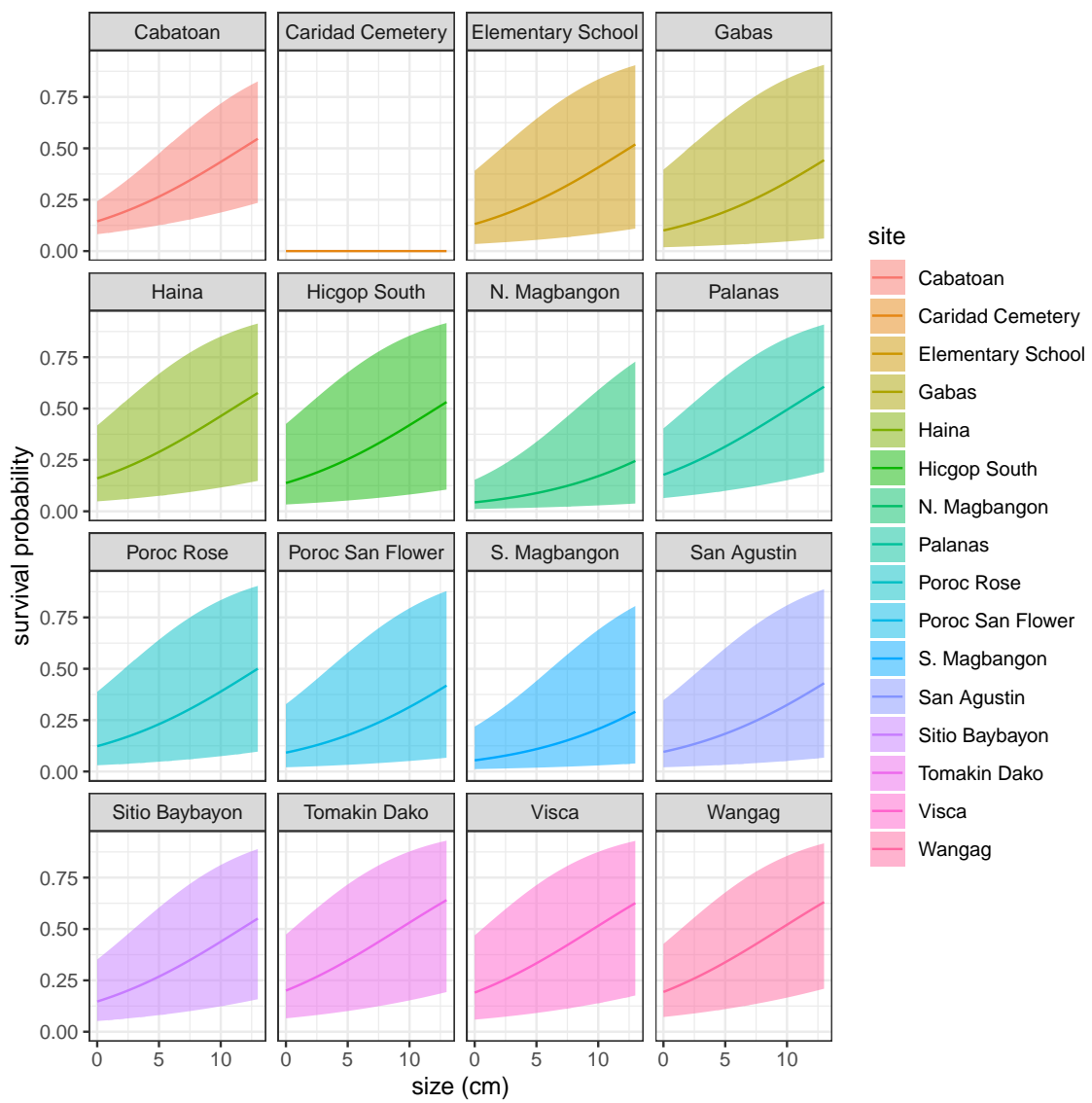


Figure B.3: Annual survival by size at each site.

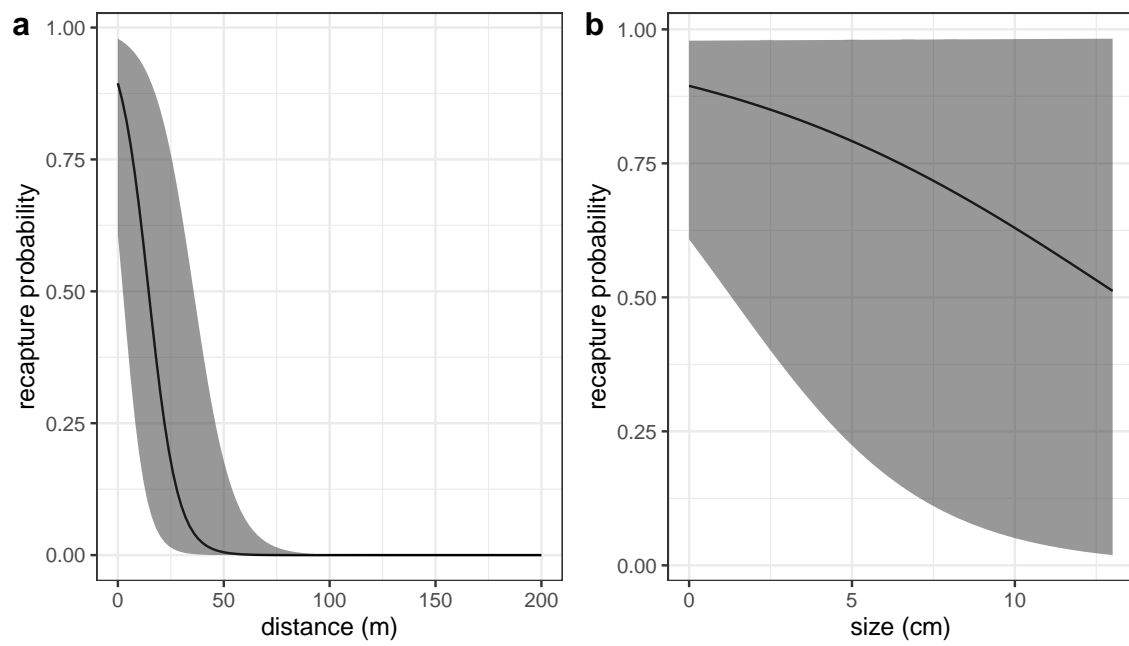


Figure B.4: Effects of a) minimum distance between divers and the anemone where the fish was first caught and b) fish size on the probability the fish will be recaptured, estimated along with survival in a mark-recapture analysis. Size has a slightly negative effect on the probability of recapture - larger fish are stronger swimmers and more likely to flee the anemone when divers approach, but with high uncertainty at larger sizes. Distance also has a negative effect on recapture, as fish tend to stay close to their anemones and are not likely to be recaptured if divers do not get close to their anemone.

C Result details and sensitivity

678 C.1 Abundance trends by site

We use the number of females captured at each site in each sampling year, scaled by the proportion of habitat sampled at that site in that year and by the probability of
681 capturing a fish, to estimate abundance trends for each site (Fig. C.1).

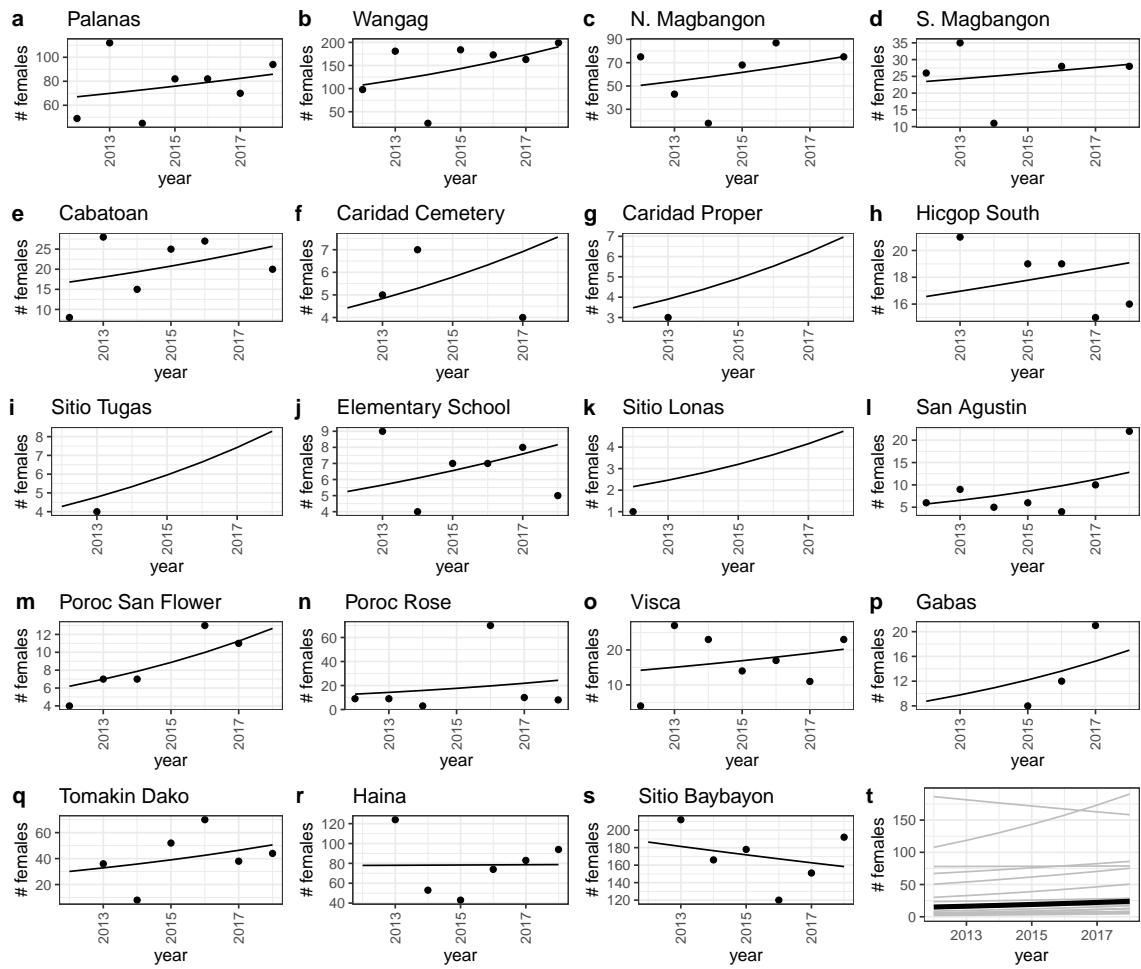


Figure C.1: Scaled number of females captured (black dots) and abundance trends (black lines) by site from a mixed effects model with site as a random effect.

C.2 Compensating for density dependence

Estimating persistence metrics without compensating for density-dependence in our
684 data gives us an understanding of whether individuals at our sites are able to replace
themselves and whether our sites persist as in isolation at the current abundance
levels, rather than at low abundance. Without compensation for early life density-
687 dependence, all of our metrics show that the set of sites we sample is less likely to
persist as an isolated network. We estimate egg-recruit survival (S_e) to be 7.8e-04
[1.2e-04, 0.033] and average lifetime recruit production (LRP) across sites to be 0.83
690 [0.28, 3.89], with XX% of LRP estimates ≥ 1 . (Fig. C.2c). Our estimate of local
replacement (LR), which estimates replacement for recruits from our sites returning
to our sites implicitly including dispersal, is 0.09 [0.03, 0.44].

693 When we calculate LR using all arriving recruits to our sites, however, rather
than just those originating there, the best estimate is > 1 (1.22, with XX% of values
with uncertainty ± 1), suggesting that there is recruit-recruit replacement at our sites
696 when we include immigrant recruits.

We do not find any sites with a best estimate or uncertainty range of $SP > 1$
(Figs. C.3a), with the exception of the wide uncertainty bounds on SP for Caridad
699 Cemetery. Our best estimate of the dominant eigenvalue of the realized connectivity
matrix λ_c is 0.21 [0.07, 0.92] with $p(\lambda \geq 1 = XX)$ (Fig. C.3c).

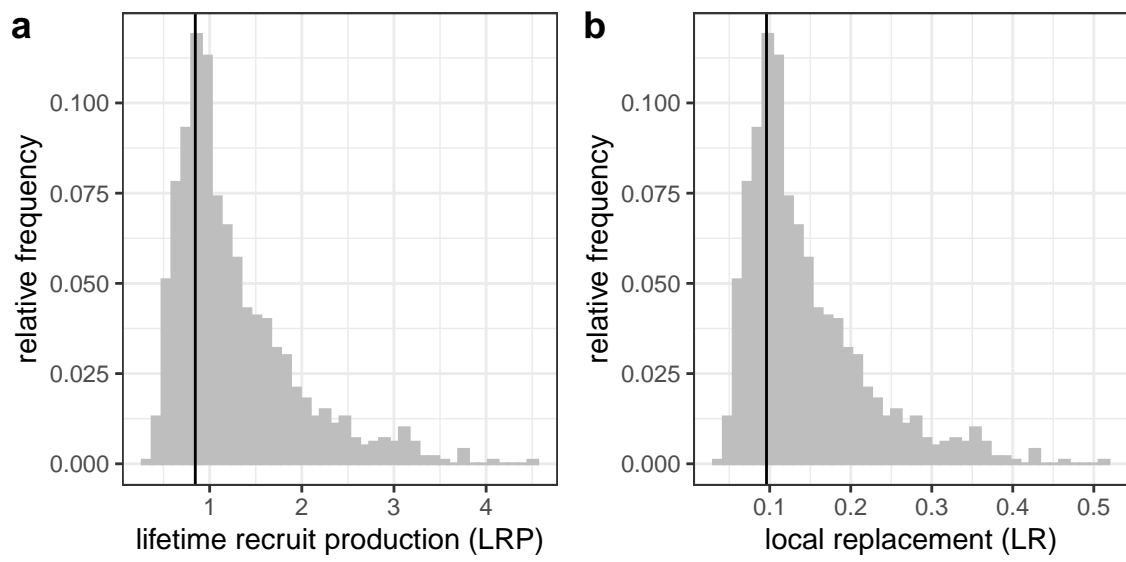


Figure C.2: Estimates of a) LRP, and b) local replacement without compensating for density dependence in early life stages in our data, showing the best estimate (black solid line) and range of estimates considering uncertainty in the inputs. These estimates compare to those in 4c,d, where we correct for additional mortality in early life due to density dependence.

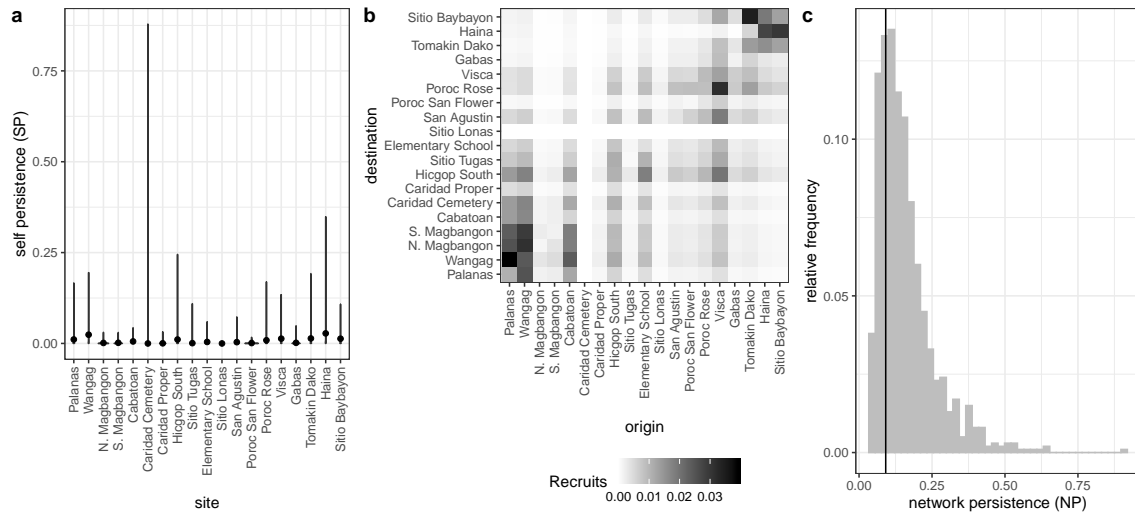


Figure C.3: Values of self-persistence (a), realized connectivity among sites (b), and network persistence (c) without compensation for density-dependence in early life stages in our data. For self-persistence (a) and network persistence (c), the best estimate is shown with in black (point for (a), line for (c)) and the range of estimates considering uncertainty is shown in grey. These estimates compare to those in 5 where we attempt to compensate for density dependence in early life stages.

C.3 LEP and LRP by site

⁷⁰² WRITE SOME TEXT!

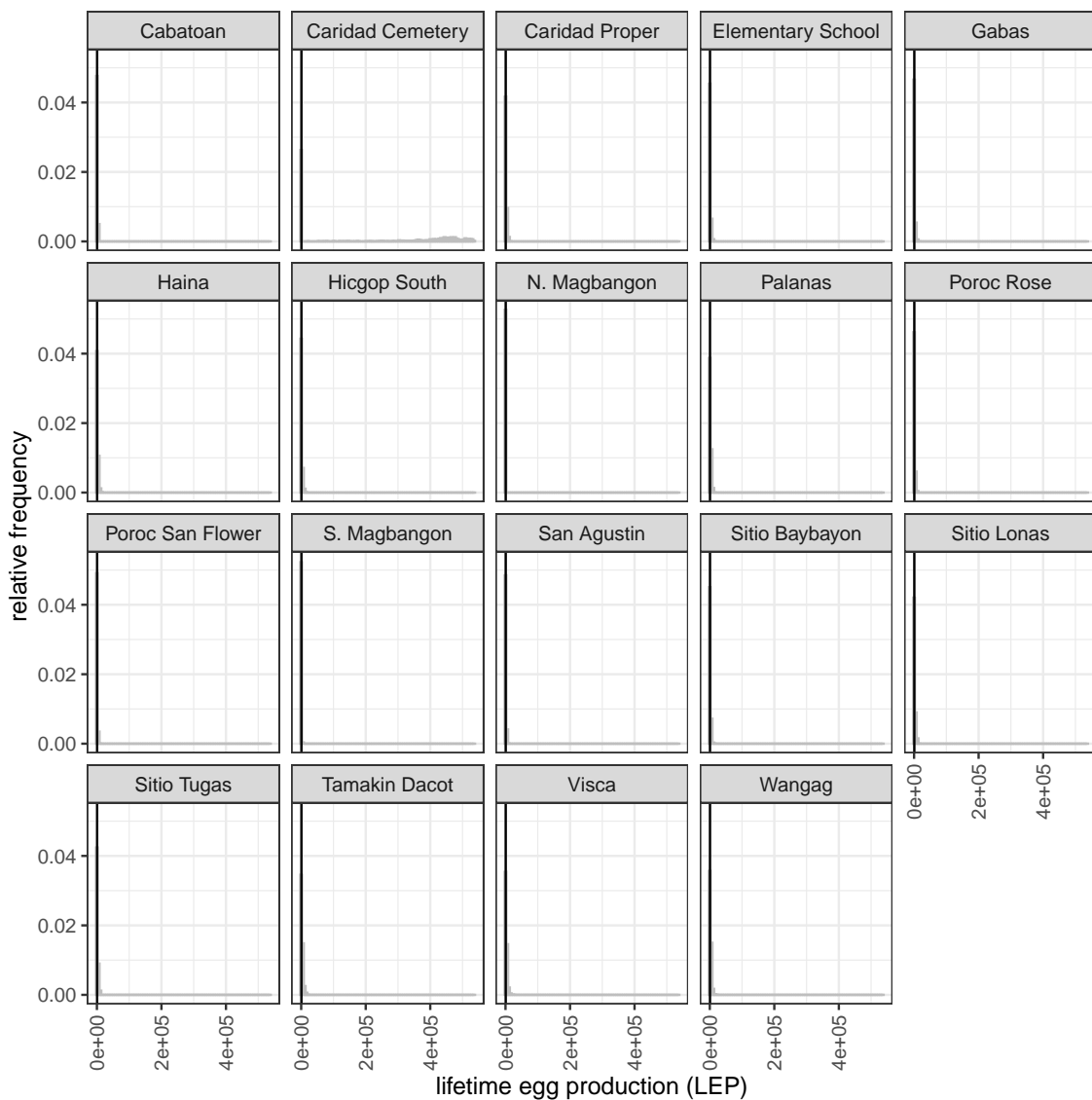


Figure C.4: Write a caption.

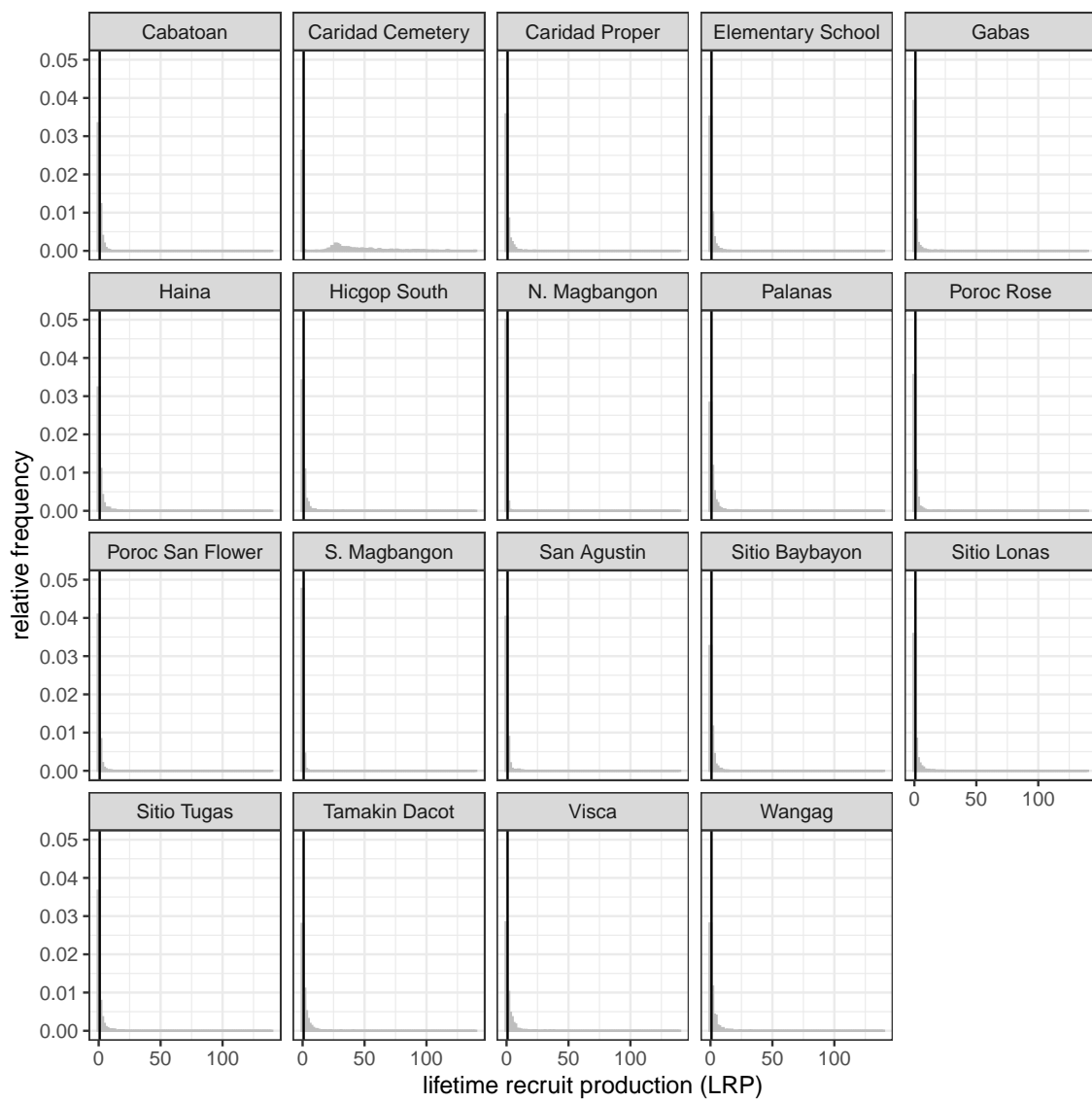


Figure C.5: Write a caption.

C.4 Sensitivity to parameters

The range of parameters not shown in the main text (Fig. 3):

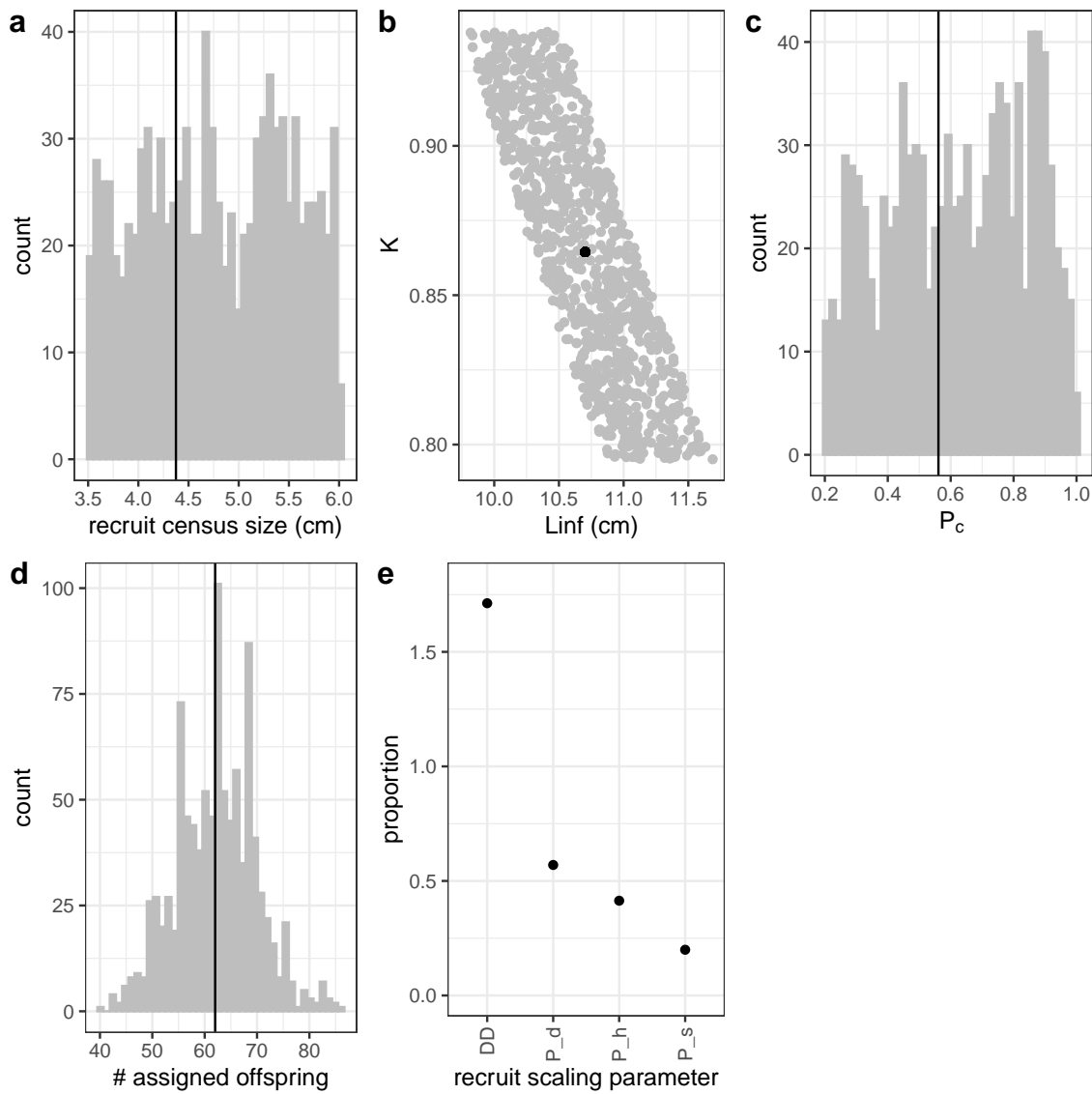


Figure C.6: Range of parameter inputs for uncertainty runs with all uncertainty included, where the black line or point is the value used for the best estimate: a) $\text{size}_{\text{recruit}}$, the census size at which fish are considered to have recruited after egg-recruit survival occurs; b) the parameters L_{∞} and K of the von Bertalanffy growth model; c) P_c , the probability of capturing a fish; d) number of offspring assigned back to parents in the parentage analysis; e) factors that scale the number of estimated recruits from our site based on density-dependence in settler success (DD), proportion of the dispersal kernel captured by our sampling region (P_d), the cumulative proportion of our sites we sampled over time (P_h), and the proportion of our sampling area that is habitat (P_s).

⁷⁰⁵ C.5 Effects of different types of uncertainty on metrics

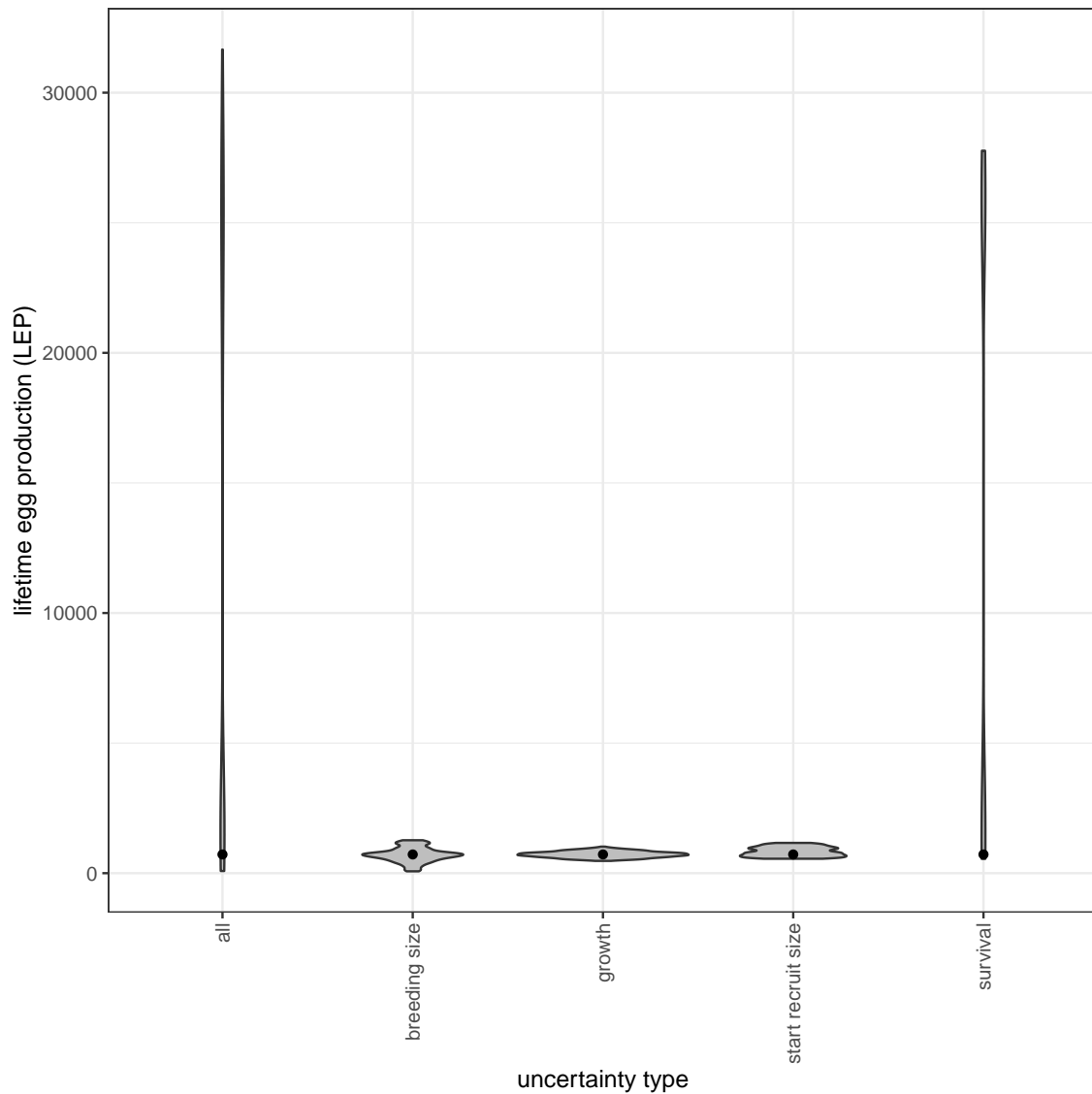


Figure C.7: The contribution of different sources of uncertainty in LEP.

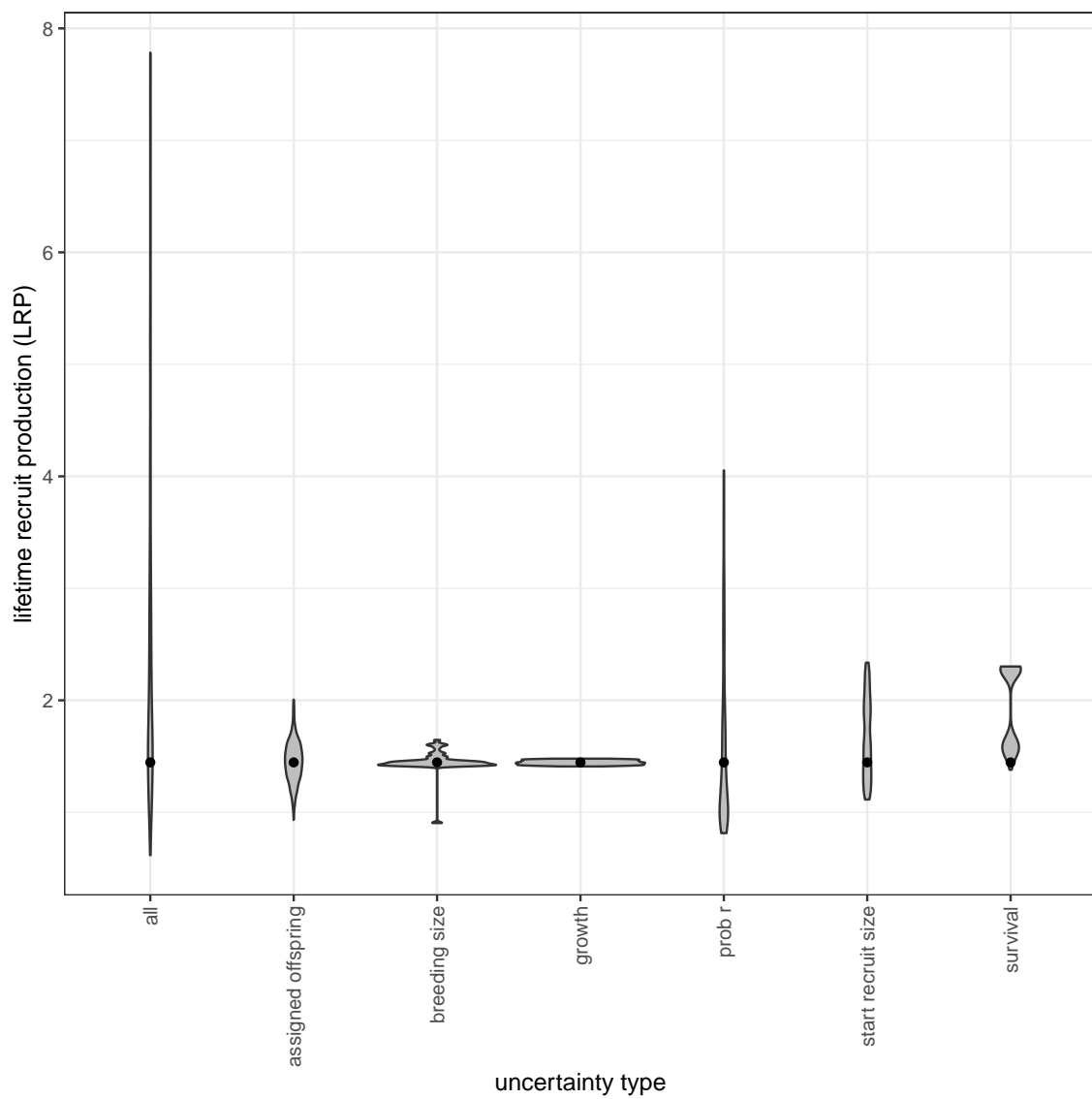


Figure C.8: The contribution of different sources of uncertainty in LRP.

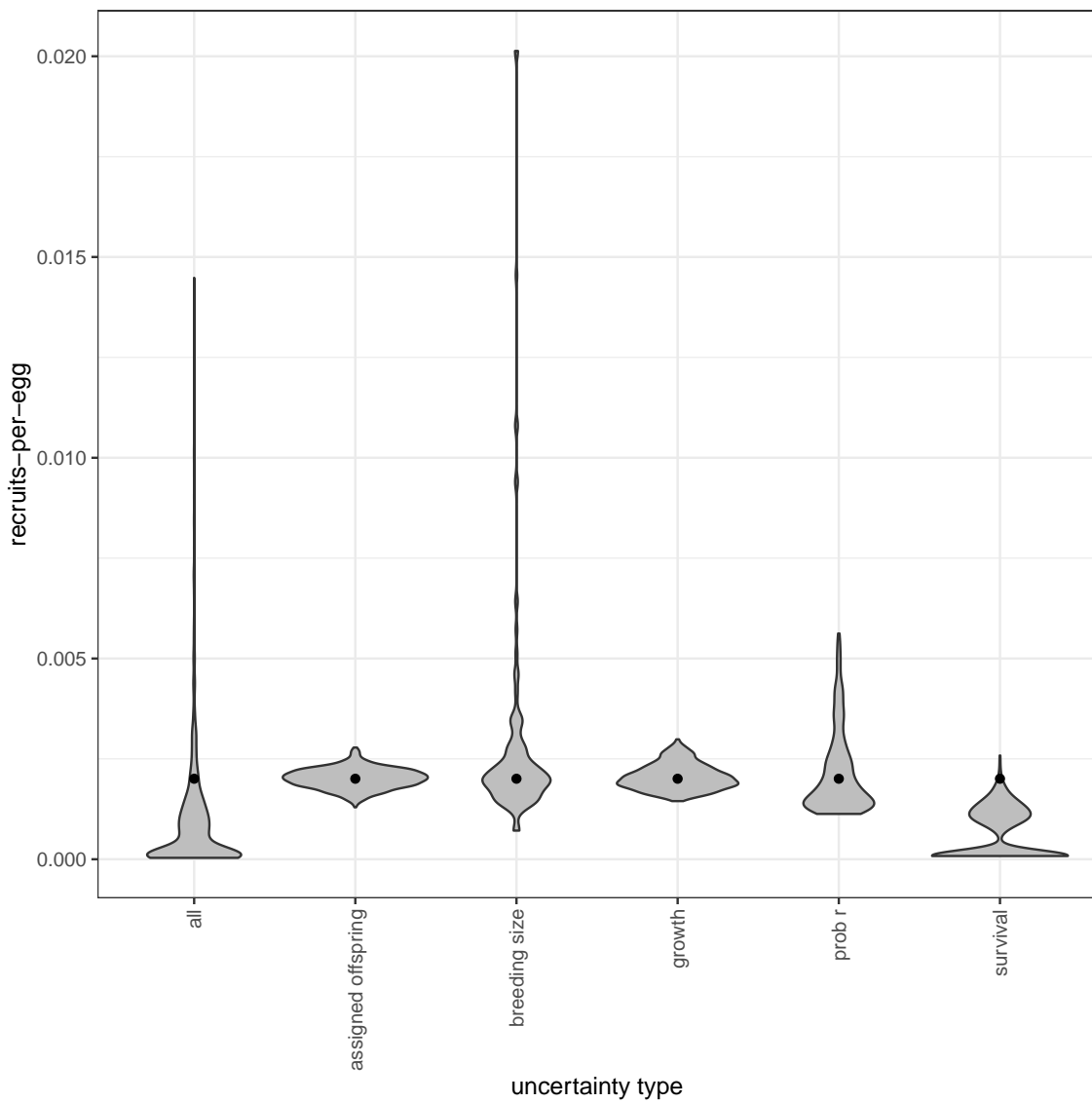


Figure C.9: The contribution of different sources of uncertainty in egg-recruit survival.

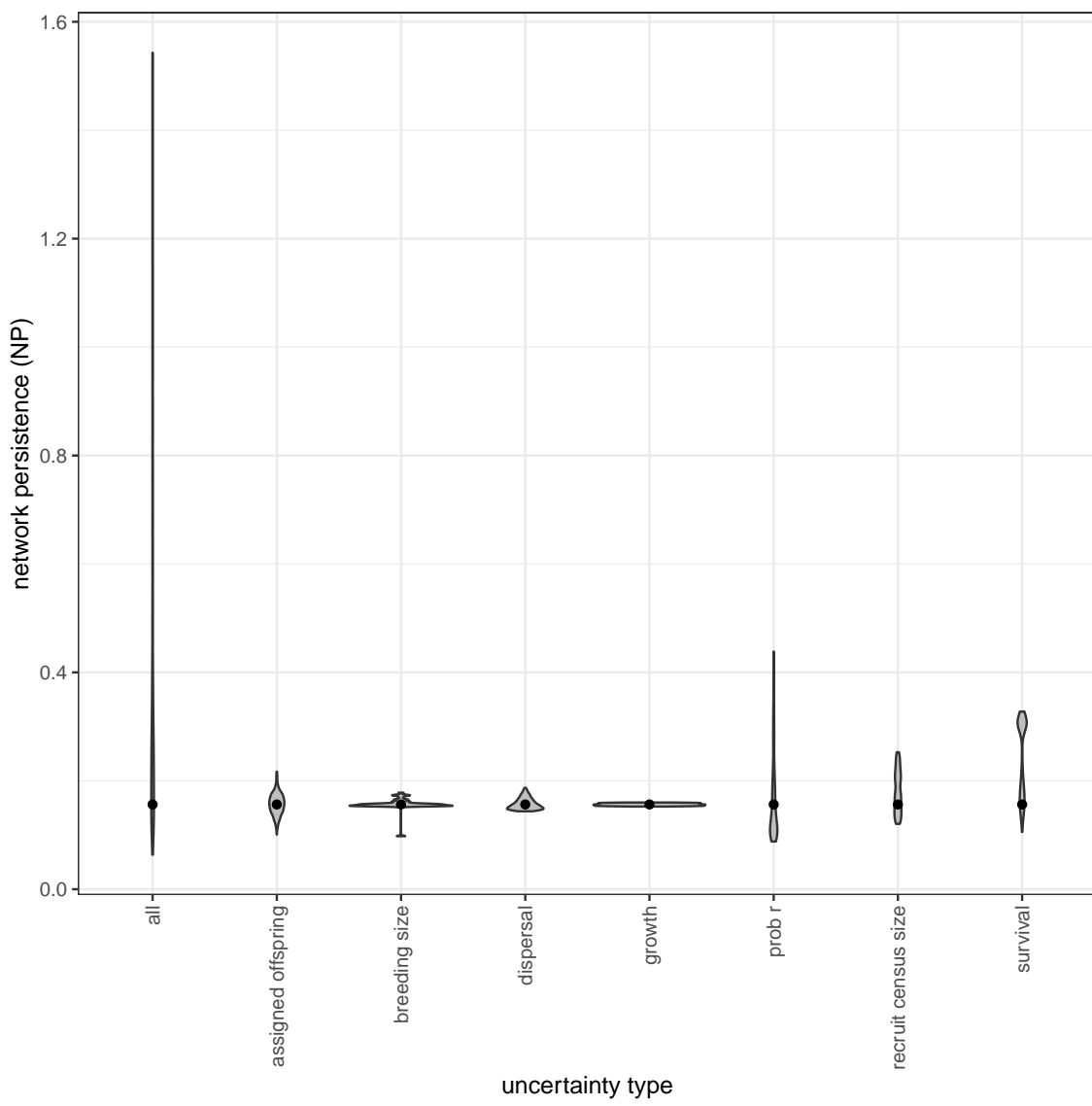


Figure C.10: The contribution of different sources of uncertainty in NP.

References

- Glenn R Almany, Serge Planes, Simon R Thorrold, Michael L Berumen, Michael
708 Bode, Pablo Saenz-Agudelo, Mary C Bonin, Ashley J Frisch, Hugo B Harrison,
Vanessa Messmer, et al. Larval fish dispersal in a coral-reef seascape. *Nature
Ecology & Evolution*, 1:0148, 2017.
- Michael Arvedlund, Mark I McCormick, Daphne G Fautin, and Mogens Bildsøe. Host
recognition and possible imprinting in the anemonefish *amphiprion melanopus*
(pisces: Pomacentridae). *Marine Ecology Progress Series*, 188:207–218, 1999.
711
- Diana S Baetscher, Eric C Anderson, Elizabeth A Gilbert-Horvath, Daniel P Malone,
Emily T Saarman, Mark H Carr, and John Carlos Garza. Dispersal of a nearshore
marine fish connects marine reserves and adjacent fished areas along an open coast.
714 *Molecular ecology*, 28(7):1611–1623, 2019.
- Douglas Bates, Martin Mächler, Ben Bolker, and Steve Walker. Fitting linear mixed-
effects models using lme4. *Journal of Statistical Software*, 67(1):1–48, 2015. doi:
720 10.18637/jss.v067.i01.
- David R Bellwood and Rebecca Fisher. Relative swimming speeds in reef fish larvae.
Marine Ecology Progress Series, 211:299–303, 2001.
- Michael Bode, David H Williamson, Hugo B Harrison, Nick Outram, and Geoffrey P
723 Jones. Estimating dispersal kernels using genetic parentage data. *Methods in
Ecology and Evolution*, 9(3):490–501, 2018.

⁷²⁶ Michael Bode, Jeffrey M. Leis, Luciano B. Mason, David H. Williamson, Hugo B. Harrison, Severine Choukroun, and Geoffrey P. Jones. Successful validation of a larval dispersal model using genetic parentage data. *PLOS Biology*, 17(7):1–13, 07 2019. doi: 10.1371/journal.pbio.3000380. URL <https://doi.org/10.1371/journal.pbio.3000380>.

⁷³² Louis W. Botsford, Alan Hastings, and Steven D. Gaines. Dependence of sustainability on the configuration of marine reserves and larval dispersal distance. *Ecology Letters*, 4:144–150, 2001.

⁷³⁵ Louis W Botsford, J Wilson White, and Alan Hastings. *Population Dynamics for Conservation*. Oxford University Press, 2019.

⁷³⁸ Scott C Burgess, Kerry J Nickols, Chris D Griesemer, Lewis AK Barnett, Allison G Dedrick, Erin V Satterthwaite, Lauren Yamane, Steven G Morgan, J Wilson White, and Louis W Botsford. Beyond connectivity: how empirical methods can quantify population persistence to improve marine protected-area design. *Ecological Applications*, 24(2):257–270, 2014.

⁷⁴¹ Peter Buston. Forcible eviction and prevention of recruitment in the clown anemonefish. *Behavioral Ecology*, 14(4):576–582, 2003a.

⁷⁴⁴ Peter Buston. Social hierarchies: size and growth modification in clownfish. *Nature*, 424(6945):145–146, 2003b.

Peter M Buston and Cassidy C DAloia. Marine ecology: reaping the benefits of local dispersal. *Current Biology*, 23(9):R351–R353, 2013.

- 747 Peter M Buston and Jane Elith. Determinants of reproductive success in dominant pairs of clownfish: a boosted regression tree analysis. *Journal of Animal Ecology*, 80(3):528–538, 2011.
- 750 Peter M Buston, Geoffrey P Jones, Serge Planes, and Simon R Thorrold. Probability of successful larval dispersal declines fivefold over 1 km in a coral reef fish. *Proceedings of the Royal Society of London B: Biological Sciences*, page rspb20112041, 2011.
- 753 Henry S Carson, Geoffrey S Cook, Paola C López-Duarte, and Lisa A Levin. Evaluating the importance of demographic connectivity in a marine metapopulation. *Ecology*, 92(10):1972–1984, 2011.
- 756 Hal Caswell. *Matrix population models: construction, analysis, and interpretation*. Sinauer Associates Inc., Sunderland, Massachusetts, 2nd edition, 2001.
- 759 Katrina A Catalano, Allison G Dedrick, Michelle Stuart, Jonathan Purtiz, Humberto Montes, Jr., and Malin Pinsky. Interannual variability of genetic connectivity in a coral reef fish *Amphiprion clarkii*. in prep.
- 762 C. C. D'Aloia, S. M. Bogdanowicz, J. E. Majoris, R. G. Harrison, and P. M. Buston. Self-recruitment in a Caribbean reef fish: a method for approximating dispersal kernels accounting for seascape. *Molecular Ecology*, 22(9):2563–2572, May 2013.
- 765 ISSN 09621083. doi: 10.1111/mec.12274. URL <http://doi.wiley.com/10.1111/mec.12274>.

- Cassidy C DAloia, Steven M Bogdanowicz, Robin K Francis, John E Majoris,
768 Richard G Harrison, and Peter M Buston. Patterns, causes, and consequences
of marine larval dispersal. *Proceedings of the National Academy of Sciences*, 112
(45):13940–13945, 2015.
- 771 JK Elliott, JM Elliott, and RN Mariscal. Host selection, location, and association
behaviors of anemonefishes in field settlement experiments. *Marine Biology*, 122
(3):377–389, 1995.
- 774 Stephen P Ellner, Dylan Z Childs, Mark Rees, et al. Data-driven modelling of
structured populations. *A practical guide to the Integral Projection Model*. Cham:
Springer, 2016.
- 777 Augustus J. Fabens. Properties and fitting of the von bertalanffy growth curve.
Growth, 29:265–289, 1965.
- Daphne Gail Fautin, Gerald R Allen, Gerald Robert Allen, Australia Naturalist,
780 Gerald Robert Allen, and Australie Naturaliste. Field guide to anemonefishes and
their host sea anemones. 1992.
- Will F Figueira. Connectivity or demography: defining sources and sinks in coral
783 reef fish metapopulations. *Ecological Modelling*, 220(8):1126–1137, 2009.
- Rebecca Fisher. Swimming speeds of larval coral reef fishes: impacts on self-
recruitment and dispersal. *Marine Ecology Progress Series*, 285:223–232, 2005.

786 Lysel Garavelli, J Wilson White, Iliana Chollett, and Laurent Marcel Chérubin. Population
models reveal unexpected patterns of local persistence despite widespread
789 larval dispersal in a highly exploited species. *Conservation Letters*, 11(5):e12567,
2018.

792 Sarah O Hameed, J Wilson White, Seth H Miller, Kerry J Nickols, and Steven G Morgan. Inverse approach to estimating larval dispersal reveals limited population
connectivity along 700 km of wave-swept open coast. *Proceedings of the Royal Society B: Biological Sciences*, 283(1833):20160370, 2016.

Ilkka Hanski. Metapopulation dynamics. *Nature*, 396(6706):41–49, 1998.

795 Hugo B Harrison, David H Williamson, Richard D Evans, Glenn R Almany, Simon R Thorrold, Garry R Russ, Kevin A Feldheim, Lynne Van Herwerden, Serge Planes, Maya Srinivasan, et al. Larval export from marine reserves and the recruitment
798 benefit for fish and fisheries. *Current biology*, 22(11):1023–1028, 2012.

801 Deborah R Hart and Antonie S Chute. Estimating von bertalanffy growth parameters from growth increment data using a linear mixed-effects model, with an application to the sea scallop *placopecten magellanicus*. *ICES Journal of Marine Science*, 66 (10):2165–2175, 2009.

804 Alan Hastings and Louis W. Botsford. Persistence of spatial populations depends on returning home. *Proceedings of the National Academy of Sciences*, 103:6067–6072, 2006.

Akihisa Hattori and Yasunobu Yanagisawa. Life-history pathways in relation to
807 gonadal sex differentiation in the anemonefish, *amphiprion clarkii*, in temperate
waters of japan. *Environmental Biology of Fishes*, 31(2):139–155, 1991.

Kina Hayashi, Katsunori Tachihara, and James Davis Reimer. Low density popu-
810 lations of anemonefish with low replenishment rates on a reef edge with anthro-
pogenic impacts. *Environmental Biology of Fishes*, 102(1):41–54, 2019.

Jordan N. Holtswarth, Shem B. San Jose, Humberto R. Montes Jr., James W. Morley,
813 and Malin. L Pinsky. The reproductive seasonality and fecundity of yellowtail
clownfish (*amphiprion clarkii*) off the philippines. *Bulletin of Marine Science*, 93,
2017.

816 Darren W Johnson, Mark R Christie, Timothy J Pusack, Christopher D Stallings,
and Mark A Hixon. Integrating larval connectivity with local demography reveals
regional dynamics of a marine metapopulation. *Ecology*, 99(6):1419–1429, 2018.

819 J.L. Laake. RMark: An r interface for analysis of capture-recapture data with
MARK. AFSC Processed Rep. 2013-01, Alaska Fish. Sci. Cent., NOAA,
Natl. Mar. Fish. Serv., Seattle, WA, 2013. URL [http://www.afsc.noaa.gov/
822 Publications/ProcRpt/PR2013-01.pdf](http://www.afsc.noaa.gov/Publications/ProcRpt/PR2013-01.pdf).

David Lecchini, Serge Planes, and René Galzin. Experimental assessment of sensory
modalities of coral-reef fish larvae in the recognition of their settlement habitat.
825 *Behavioral Ecology and Sociobiology*, 58(1):18–26, 2005.

Dale R Lockwood, Alan Hastings, and Louis W Botsford. The effects of dispersal patterns on marine reserves: does the tail wag the dog? *Theoretical population biology*, 61(3):297–309, 2002.

Haruki Ochi. Mating behavior and sex change of the anemonefish, amphiprion clarkii, in the temperate waters of southern japan. *Environmental Biology of Fishes*, 26(4):257–275, 1989.

Malin L Pinsky, Humberto R Montes Jr, and Stephen R Palumbi. Using isolation by distance and effective density to estimate dispersal scales in anemonefish. *Evolution*, 64(9):2688–2700, 2010.

BJ Puckett and DB Eggleston. Metapopulation dynamics guide marine reserve design: importance of connectivity, demographics, and stock enhancement. *Ecosphere*, 7(6), 2016.

H Ronald Pulliam. Sources, sinks, and population regulation. *The American Naturalist*, 132(5):652–661, 1988.

Océane C Salles, Glenn R Almany, Michael L Berumen, Geoffrey P Jones, Pablo Saenz-Agudelo, Maya Srinivasan, Simon R Thorrold, Benoit Pujol, and Serge Planes. Strong habitat and weak genetic effects shape the lifetime reproductive success in a wild clownfish population. *Ecology letters*, 23(2):265–273, 2020.

Ocane C. Salles, Jeffrey A. Maynard, Marc Joannides, Corentin M. Barbu, Pablo Saenz-Agudelo, Glenn R. Almany, Michael L. Berumen, Simon R. Thorrold, Geoffrey P. Jones, and Serge Planes. Coral reef fish populations can persist without

immigration. *Proceedings of the Royal Society B: Biological Sciences*, 282(1819): 20151311, November 2015. ISSN 0962-8452, 1471-2954. doi: 10.1098/rspb.2015.

849 1311. URL <http://rspb.royalsocietypublishing.org/lookup/doi/10.1098/rspb.2015.1311>.

Diane M Thompson, J Kleypas, F Castruccio, Enrique N Curchitser, Malin L Pinsky,
852 B Jönsson, and James R Watson. Variability in oceanographic barriers to coral
larval dispersal: Do currents shape biodiversity? *Progress in oceanography*, 165:
110–122, 2018.

855 Nick Tolimieri and Phillip S Levin. The roles of fishing and climate in the population
dynamics of bocaccio rockfish. *Ecological Applications*, 15(2):458–468, 2005.

Jinliang Wang. Sibship reconstruction from genetic data with typing errors. *Genetics*,
858 166(4):1963–1979, 2004.

Jinliang Wang. Estimation of migration rates from marker-based parentage analysis.
Molecular ecology, 23(13):3191–3213, 2014.

861 J. Wilson White, Mark H Carr, Jennifer E Caselle, Libe Washburn, C. Brock Wood-
son, Stephen R Palumbi, Peter M Carlson, Robert R Warner, Bruce A Menge,
John A Barth, Carol A Blanchette, Peter T Raimondi, and Kristen Milligan. Con-
nectivity, dispersal, and recruitment: Connecting benthic communities and the
864 coastal ocean. *Oceanography*, 32(3):50–59, 2019.

Jw White, Lw Botsford, A Hastings, and Jl Largier. Population persistence in ma-
867 rine reserve networks: incorporating spatial heterogeneities in larval dispersal.

Marine Ecology Progress Series, 398:49–67, January 2010. ISSN 0171-8630, 1616-1599. doi: 10.3354/meps08327. URL <http://www.int-res.com/abstracts/meps/v398/p49-67/>.

Adam Yawdoszyn. Fecundity in clownfish. in prep.